

Carpal Kinematics During Functional Tasks: A 3-D *In Vivo* Analysis of Simulated
Hammering and Carpal Distraction

By

Evan L. Leventhal

Sc.B., Brown University, 2003

Submitted in partial fulfillment of the requirements for the degree of Doctor of
Philosophy in the Program in Biomedical Engineering at Brown University

Providence, Rhode Island

May 2009

© Copyright 2009 by Evan Leventhal

This dissertation by Evan Leventhal is accepted in its present form
by the Department of Biomedical Engineering as satisfying the
dissertation requirement for the degree of Doctor of Philosophy.

Date_____

Joseph J. Crisco, Ph.D., Advisor

Date_____

Edward Akelman, M.D., Reader

Date_____

Braden C. Fleming, Ph.D., Reader

Date_____

David H. Laidlaw, Ph.D., Reader

Date_____

Scott W. Wolfe, M.D.,
External Reader

Approved by the Graduate Council

Date_____

Sheila Bonde,
Dean of the Graduate School

Curriculum Vitae

Evan Leventhal was born on August 31st, 1981 in Manhasset, NY to Gary and Roberta Leventhal. Evan was raised in East Hills, NY with his younger sister, Caryn. He graduated from Roslyn High School in 1999. In high school, Evan joined Rescue Hook & Ladder Co. #1 of Roslyn, NY and trained as a firefighter and emergency medical technician. He received his Bachelor in Science in Computer Science from Brown University in May 2003. While at Brown, Evan was the varsity coxswain for the Men's Crew Team, and competed in the 2001 Princeton FISA World Cup winning a bronze medal. After college, Evan started medical school at (what was then named) Brown Medical School and subsequently joined the MD/PhD program during his second year.

Resume

Evan L. Leventhal

Brown University
Box G-8237
Providence, RI 02912
516.236.1876
Evan_Leventhal@brown.edu

16 Melby Lane
East Hills, NY 11576
516.484.5600

EDUCATION

Expected 2011 M.D. Brown Medical School, Providence RI

Expected 2009 Ph.D. Bioengineering. Brown University, Providence RI

2003 Sc.B. Computer Science. Brown University, Providence, RI
GPA 3.7 (in major)

1999 Roslyn High School, Roslyn Heights, NY

RESEARCH EXPERIENCE

1997 Long Island Jewish Hospital, Department Radiation Oncology
1998 Cold Spring Harbor Laboratories
2004-Present Bioengineering Laboratory,
Department of Orthopaedics, Brown Medical School
In Vivo carpal bone kinematics.
Shoulder rotator cuff injury.

PUBLICATIONS

Leventhal EL, Wolfe SW, Walsh, EF, Crisco JJ. Computer Optimized Screw Placement for Volar Percutaneous Scaphoid Fracture Fixation, Journal of Hand Surgery. (in press)

Leventhal EL, Moore DC, Akelman E, Weiss A-PC, Wolfe SW, Crisco JJ. Interfragmentary Motion in Patients with Scaphoid Nonunions, Journal of Hand Surgery, 2009;31(5):391-400.

Calfee RP, **Leventhal EL**, Wilkerson JA, Moore DC, Akelman E, Crisco JJ. Simulated Radioscapholunate Fusion Alters Carpal Kinematics While Preserving Dart Thrower's Motion, Journal of Hand Surgery, 2008;33(4):503-10.

Tocci SL, Tashjian RZ, **Leventhal E**, Spenciner DB, Green A, Fleming BC: Biomechanical evaluation of single row arthroscopic rotator cuff repair (ARCR) technique. Journal of Shoulder & Elbow Surgery, 2008;17(5):808-14.

Bowers ME, Tung GA, Trinh N, **Leventhal E**, Crisco JJ, Kimia B, Fleming BC. Effects of ACL interference screws on articular cartilage volume and thickness measurements with 1.5 T and 3 T MRI., Osteoarthritis Cartilage, 2008;16(5):572-8.

Tashjian RZ, **Leventhal E**, Spenciner DB, Green A, Fleming BF. Initial Fixation Strength of Massive Rotator Cuff Tears, *Arthroscopy*, 2007;23(7):710-6.

Moore DC, Crisco JJ, Trafton TG, **Leventhal EL**. A digital database of wrist bone anatomy and carpal kinematics. *J Biomech*, 2007;40(11):2537-42.

ABSTRACTS/PRESENTATIONS

Orr CM, **Leventhal EL**, Chivers FS, Menzies SL, Larson S, Crisco JJ. "Three-dimensional midcarpal kinematics during wrist extension in five anthropoid species." Submitted to annual meeting of the American Association of Physical Anthropologist, Chicago, IL, 2009.

Leventhal EL, Moore DC, Akelman E, Wolfe SW, Crisco JJ. "Midcarpal Joint Motion Dominates Carpal Motion During a Simulated Hammering Task." 55th Annual Meeting of the Orthopaedic Research Society (ORS), Las Vegas, NV, February 22-25, 2009.

Leventhal EL, Moore DC, Akelman E, Wolfe SW, Crisco JJ. "Changes at the Radiocarpal and Midcarpal Joints with Wrist Distraction." 55th Annual Meeting of the Orthopaedic Research Society (ORS), Las Vegas, NV, February 22-25, 2009.

Orr CM, **Leventhal EL**, Chivers FS, Crisco JJ. "Kinematics of the os centrale in *Pongo pygmaeus*: implications for the knuckle-walking hominin ancestor hypothesis." Invited presentation for symposium entitled "Evolution of hominin bipedalism: new perspectives". Abstract in *American Journal of Physical Anthropology Suppl* 46:166.

Leventhal EL, Wolfe SW, Walsh, EF, Crisco JJ. "Ideal Screw Axis Computation for Acute Scaphoid Fracture Fixation" 34th Annual Northeast Bioengineering Conference, Providence, RI, April 4-6, 2008.

Leventhal EL, Wolfe SW, Walsh, EF, Crisco JJ. "Ideal Screw Placement for Volar Percutaneous Scaphoid Fixation" 75th Annual Meeting of the American Academy of Orthopaedic Surgeons (AAOS), San Francisco, CA, March 5-9, 2008.

Leventhal EL, Wolfe SW, Walsh, EF, Crisco JJ. "Computer Optimized Screw Placement for Volar Percutaneous Scaphoid Fracture Fixation" 54th Annual Meeting of the Orthopaedic Research Society (ORS), San Francisco, CA, March 2-5, 2008.

Calfee RP, **Leventhal EL**, Wilkerson JA, Moore DC, Akelman E, Crisco JJ. "Simulated Radioscapholunate Fusion Alters Carpal Kinematics While Preserving Dart Thrower's Motion" 54th Annual Meeting of the Orthopaedic Research Society (ORS), San Francisco, CA, March 2-5, 2008.

Sharp WK, Moore DC, **Leventhal EL**, Aslani K, Badger GJ, Fleming BF. "Variations in the Thickness of the Subchondral Bone Plate and the Apparent Trabecular Density of the Goat Femoral Condyle" 54th Annual Meeting of the Orthopaedic Research Society (ORS), San Francisco, CA, March 2-5, 2008.

Bowers ME, Fleming BC, Tung GA, **Leventhal EL**, Trinh N, Crisco JJ, Kimia B,. “Effects of ACL Interference Screws on Articular Cartilage Thickness Measurements with 1.5T and 3T MRI” American Society of Biomechanics, Palo Alto, CA, August 22-25, 2007.

Fleming BC, Bowers ME, Tung GA, **Leventhal EL**, Trinh N, Crisco JJ, Kimia B,. “Effects of ACL Interference Screws on Femorotibial Cartilage Thickness Measurements using 1.5T and 3T MRI. Poster presentation” Workshop on Imaging-Based Measures of Osteoarthritis, Salzburg, Austria, July 11-14, 2007.

Tocci SL, Tashjian R, **Leventhal EL**, Spenciner D, Green A, Fleming BC. “Biomechanical Evaluation of Single Row Arthroscopic Rotator Cuff Repair (ARCR) Technique” 74th Annual Meeting of the American Academy of Orthopaedic Surgeons (AAOS), San Diego, CA, February 14-18, 2007.

Tocci SL, Tashjian R, **Leventhal EL**, Spenciner D, Green A, Fleming BC. “Biomechanical Evaluation of Single Row Arthroscopic Rotator Cuff Repair Technique Versus Open Transosseous Repair Technique” 53rd Annual Meeting of the Orthopaedic Research Society (ORS), San Diego, CA, February 11-14, 2007.

Tashjian RZ, **Leventhal EL**, Spenciner D, Green A, Fleming BC. “Initial Fixation Strength of Repairs of Massive Rotator Cuff Tears”. 73rd Annual Meeting of the American Academy of Orthopaedic Surgeons (AAOS), Chicago IL, March 22-26, 2006.

Tashjian RZ, **Leventhal E**, Spenciner D, Green A, Fleming BC. “Initial Fixation Strength of Repairs of Massive Rotator Cuff Tears”. 52nd Annual Meeting of the Orthopaedic Research Society (ORS), Chicago IL, March 19-22, 2006.

Leventhal EL, Moore DC, Akelman E, Weiss A-PC, Wolfe SW, Crisco JJ. “Interfragmentary Motion in Patients with Scaphoid Nonunions.” 52nd Annual Meeting of the Orthopaedic Research Society (ORS), Chicago IL, March 19-22, 2006.

Moore DC, Wilkerson JA, Calfee RP, Crisco JJ, **Leventhal EL**, Akelman E. “Fidelity of *In Vitro* and *In Vivo* Radiocarpal Kinematic Data.” 52nd Annual Meeting of the Orthopaedic Research Society (ORS), Chicago IL, March 19-22, 2006.

AFFILIATIONS

American Medical Student Association
American Medical Association
Orthopaedic Research Society
Osteoarthritis Research Society International
American Physician Scientists Association

SPORTS/INTERESTS

Brown Crew Team. Four year varsity athlete.
Bronze medal 2001 Princeton FISA World Cup.
Triathlons; Skiing; Rock climbing; SCUBA Diving; EMT

Preface and Acknowledgements

Any acknowledgments must start with my loving family. To Mom, Dad and Caryn, you all have always been there for me with unconditional love and support. An extra thank you to Mom for always supplying me with endless amounts of food, even when I said no. To Silvia, for supporting me through both the highs and lows, and for always keeping a healthy supply of furry animals around. Thank you Harper, for always greeting me with a wagging tail no matter how bad my day.

I would like to thank all of the members of my committee: Dr. Edward Akelman, Dr. Braden Fleming, Dr. David Laidlaw and Dr. Scott Wolfe. Each one provided valuable insight and advice across their different areas of expertise. Their feedback and comments on my research were instrumental. I would especially like to thank my advisor, Dr. Joseph Crisco, without whom I never would have started my research career. Thank you Trey, for giving me the room to grow and providing me the gentle guidance when needed.

A special thank you to Douglas Moore, without whom I would likely still be working on my first paper. Throughout my time at the lab Doug was instrumental in moving things along. From obtaining IRB approval to editing manuscripts, Doug was always willing to take the time to help. Countless hours were spent in Doug's office with him helping me working on a paper or simply providing good conversation. Doug could always be counted on for cheerful comment to brighten one's day.

I am forever grateful to all my colleagues in the lab, past and present, who made my time there so enjoyable. It was all of you who made the lab fun. I would also like to thank Dr. Michael Ehrlich and the rest of the Department of Orthopaedics for all of their support.

Table of Contents

Chapter 1 – Introduction	1
1.1 Introduction.....	1
1.2 Background	4
1.2.1 Carpal Anatomy	4
1.2.2 Carpal Kinematics.....	5
1.2.3 The Dart Throwing Motion.....	6
1.2.4 Total Wrist Arthroplasty	7
1.2.5 Markerless Bone Registration.....	8
1.3 Carpal and Forearm Kinematics During a Simulated Hammering Task	10
1.3.1 Hammering	10
1.3.2 Static vs. Dynamic Hammering	11
1.3.3 Relevance.....	11
1.4 Conformational Changes in the Carpus During Finger Traps Distraction	13
1.4.1 Carpal Loading.....	13
1.4.2 Clinical Relevance	14
1.4.3 Computer Models.....	15
1.5 Specific Aims.....	17
1.6 References.....	19
Figures.....	23
Chapter 2 – Carpal and Forearm Kinematics During a Simulated Hammering Task	27
2.1 Abstract.....	27
2.1.1 Introduction.....	27
2.1.2 Methods.....	28
2.1.3 Results.....	28
2.1.4 Conclusion	28
2.2 Introduction.....	29
2.3 Methods.....	31
2.3.1 Volunteer Selection and CT Scanning.....	31
2.3.2 Kinematic Analysis.....	31
2.3.3 Pronation/Supination Kinematics	32
2.3.4 Data Analysis.....	33
2.3.3 Statistical Analysis.....	34
2.4 Results	36
2.4.1 Wrist and Forearm Motion.....	36
2.4.2 Radiocarpal Motion	36
2.5 Discussion.....	38
2.6 References.....	43
Figures.....	45
Chapter 3 – Conformational Changes in the Carpus During Finger Traps Distraction.....	51

3.1	Abstract	51
3.1.1	Introduction	51
3.1.2	Methods	51
3.1.3	Results	52
3.1.4	Conclusion	52
3.2	Introduction	53
3.3	Methods	56
3.3.1	Volunteer Recruitment and CT Scanning	56
3.3.2	Carpal Tracking	56
3.3.3	Outcome Variables	58
3.3.3.1	Bone Centroid Displacement	58
3.3.3.2	Centroid Distances	59
3.3.3.3	Joint Separation	59
3.3.4	Statistics	60
3.4	Results	61
3.4.1	Wrist Position and Carpal Rotation	61
3.4.2	Bone Translation	61
3.4.3	Centroid Distances	61
3.4.4	Joint Separation	62
3.5	Discussion	63
3.6	References	69
	Figures	72
	Tables	75
	Chapter 4 – Conclusions & Future Directions	78
4.1	Conclusions	78
4.1.1	What is the Dart Throwing Motion?	80
4.1.2	Intersubject Variability	81
4.2	Future Methods for Non-Invasively Measuring 3-D Carpal Kinematics	83
4.2.1	Current Research Methodologies	83
4.2.2	Future Imaging Modalities	84
4.3	Future Directions	86
4.3.1	Correlations Between Morphology and Kinematics	86
4.3.2	High Accuracy Study of a Single Specimen	87
4.4	Ongoing Loading Studies	89
4.4.1	Tensive Gripping Task	89
4.4.1.1	Background	89
4.4.1.1	Data Collection	90
4.4.2	Compressive Task	90
4.4.2.1	Background	90
4.4.2.1	Data Collection	91
4.5	References	92

List of Tables

Chapter 3

Table 3.1 Bone-bone interactions were measured as the change in distance between centroids after loading.....	76
Table 3.2 Translation vectors were calculated for each bone centroid representing its translation after loading. These vectors were represented as both a magnitude and by the orientation of the vector.....	78

List of Figures

Chapter 1

Figure 1.1	Volar view of a right wrist (MC = Metacarpal).	23
Figure 1.2	Volar view of a right wrist highlighting the proximal row (scaphoid, lunate, triquetrum and pisiform) in orange and the distal row (trapezium, trapezoid, capitate and hamate) in blue.	24
Figure 1.3	Volar view of a right wrist highlighting the three columns in the original columnar theory as proposed by Navarro (ref). In this model, the central column is composed of the lunate, capitate and hamate (orange); the medial column is composed of the triquetrum and pisiform (blue); and the lateral column is composed of the scaphoid, trapezium and trapezoid (magenta).	25
Figure 1.4	Wrist position is conventionally described in two orthogonal directions: flexion/extension and radial/ulnar deviation.	26

Chapter 2

Figure 2.1	Drawing of the hammering jig used during CT scanning. The dominant hand of each subject was supported by a forearm rest. To minimize motion during scanning, the jig was equipped with stops for the hammer handle at each of the 5 hammering positions. Each stop was a 4" long, ½" diameter dowel. The head of the hammer was removed prior to scanning, and was included in the figure for illustration purposes.	45
Figure 2.2	Wrist positions during hammering followed a path from radial-extension to ulnar-flexion, a motion also referred to as the Dart Thrower's path. These positions were normalized such that the neutral hammering position of each subject was located at the (N) average neutral hammering position for visualization purposes only.	46
Figure 2.3	There was minimal pronation/supination during hammering. Each subject rotated on average only 12° throughout the entire range of motion.	47
Figure 2.4	During hammering scaphoid and the lunate rotation was 40% and 41% of wrist motion respectively.	48
Figure 2.5	a) Each subject's path of wrist motion, or the coupling ratio, affected that subject's amount of residual radioscaphoid rotation during hammering. Radioscaphoid rotation was minimized at a path of 32° from the sagittal plane; as subjects moved away from that DTM, radioscaphoid rotation increased. b) These results were similar to those of Werner et al. (adapted from Werner et al.)	49
Figure 2.6	a) Increasing amount of flexion/extension in paths of global wrist lead to a decrease in the amount of radiolunate rotation. b) When compared to the results of Werner <i>et al.</i> , it suggests that the hammering paths of our subjects were too far towards radial/ulnar deviation to detect the path which minimizes radiolunate rotation. (adapted from Werner <i>et al.</i>)	50

Chapter 3

- Figure 3.1 Volar (left) and Radial (right) view of a single subject's wrist showing the radius, ulna, scaphoid, lunate and capitate. The centroid (red) for each carpal bone in the unloaded position, and the centroid displacement for each subject (light red) showing the translation of the subject as a function of loading. The vector representing average translation with loading is shown in green.....72
- Figure 3.2 Volar (left) and Radial (right) view of a single wrist showing the centroid (red sphere) of each bone in the unloaded position and a vector representing the average centroid displacement after loading.73
- Figure 3.3 Volar view of a single wrist in the unloaded (left) and loaded (right) state. The centroid of each bone is shown (red sphere). Intercentroid combinations that were analyzed are represented as lines connecting the two bone centroids. There is visible distraction at the radiocarpal and midcarpal joints.74
- Figure 3.4 Tensive loading caused a significant (*) increase in the interbone distances at the radioscapoid, radiolunate and lunocapitate joints. There was a non-significant increase in the interbone distance at the 3rd carpal-metacarpal joint.75

Chapter 1

Introduction

1.1 Introduction

Located between the forearm and the hand, the human wrist serves many functions and is subject to a wide range of injuries. Because the wrist, or carpus, is both complicated and poorly understood, knowledge of its kinematics would benefit both basic scientists and clinicians. Clinicians frequently treat the roughly 2 million individuals suffering from occupationally related wrist and hand arthritis in the United States (1). By improving our understanding of the function of the healthy wrist, we hope to better understand the effects of misalignment, malunion and nonunion related to the progression to degenerative osteoarthritis. This research could be applied towards designing the next generation of total wrist prostheses, which have thus far had high complication rates. In addition to treating wrist injury, improved understanding could prevent injury by helping in the design of more ergonomic tools and industrial equipment. Basic scientists who study the wrist are interested in understanding and developing computer models of the

wrist. Accurate computer models could allow us to better understand disease states and predict the functional outcomes of surgical procedures.

Most of what is known about the wrist has been derived from normal range-of-motion data and low demand tasks. The carpus has historically been challenging to study due to the small size of the carpal bones and their compact arrangement. Most common techniques for measuring kinematics have limited application in the wrist. For example, surface markers are unable to track individual bones, and invasive markers can alter the motions being studied. It is only in the last decade that the technology has existed for measuring the *in vivo* motions of the carpus without markers.

Our understanding of carpal kinematics is likely shaped by a history of measuring the wrist in the orthogonal directions of flexion/extension and radial/ulnar deviation. However, it has been hypothesized that an oblique wrist motion from radial extension to ulnar flexion is a more physiologic motion. Called the Dart Throwing Motion (DTM), this motion has been shown to play an important role in daily function and is used in a variety of activities. Studies have shown that radiocarpal motion is reduced during the DTM, but this has never been confirmed during an actual functional task. One goal of this research was to measure the *in vivo* 3-D kinematics of the wrist and forearm during a functional task that is purported to use the DTM. A simulated hammering task was chosen, as hammering is a dominant task of modern man and is an important functional motion.

In addition to unloaded motion, the wrist is often subject to loading, most commonly during pushing or pulling. All kinematic studies to date on the loading of the wrist have been performed in cadavers or were limited in their measurements. By not

studying the wrist under these loaded conditions, our knowledge of carpal kinematics is incomplete. The second goal of this research was to measure the *in vivo* effect of a tensile distractive load on the conformation of the carpus.

1.2 Background

The human carpus is required to perform a wide variety of daily tasks. With the ability to rotate with two principal degrees of freedom (flexion/extension and radial/ulnar deviation) and partially a third degree of rotational freedom (pronation/supination) (2), the wrist has a large range of motion (3), almost 70% of which is used regularly (4). The wrist is heavily involved in essential tasks such as personal hygiene, eating, and opening doors, as well as those of our earlier ancestors such as spear throwing, clubbing and hammering.

Wrist injuries are common. Traumatic injuries of the wrist are dominated by bone fracture and ligament tears, both of which have been shown to alter normal kinematics (5-7). It is well established that altered kinematics accelerates the onset of degenerative osteoarthritis (OA) (8-12). In the wrist, this pattern has been best documented in patients exhibiting the “SLAC” (scapholunate advanced collapse) pattern of wrist arthritis (9, 11). In the SLAC wrist, the articulation of the scaphoid is altered, resulting in decreased joint contact and increased contact pressure. Increased contact pressure leads to visible thinning of cartilage and further alters normal kinematics. Eventually, these degenerative changes spread throughout the wrist, ultimately requiring surgical intervention. Chronic injuries such as Kienbock’s disease have also been shown to alter normal wrist kinematics (13), and are known to progress to OA with debilitating results (14).

1.2.1 Carpal Anatomy

The wrist is a uniquely complex joint. Composed of 8 small multi-articular bones, the wrist is situated between the radius and ulna of the forearm and the five metacarpals of the palm (**Figure 1.1**). The carpus is an almost entirely passive joint, with only a portion of a single tendon from the carpi ulna extensor inserting on the hook of the hamate and the pisiform. The remaining tendons controlling wrist motion insert on the metacarpals and phalanges.

1.2.2 Carpal Kinematics

Despite more than 100 years of research (15), the kinematics of the human wrist remains poorly understood. The human carpus has been classically described by anatomists as being composed of two horizontal rows: a proximal row composed of the scaphoid, lunate, triquetrum and pisiform; and a distal row composed of the trapezium, trapezoid, capitate and hamate (**Figure 1.2**). While it is convenient to discuss the carpal bones based on this logical arrangement, this classification is less relevant when discussing kinematics.

In 1921, Navarro (16) first proposed his columnar theory, whereby the wrist was subdivided into three columns. He described a central column composed of the lunate, capitate and the hamate; a medial column composed of the triquetrum and pisiform; and a lateral column composed of the scaphoid, trapezium and trapezoid (**Figure 1.3**). This theory was later modified by Taleisnik (17), who reclassified the trapezium and trapezoid as being part of the central column. In this modified version, the lateral column consisted of only the scaphoid. Both columnar theories describe the central column moving

together during flexion/extension and the medial and lateral columns rotating about the central column during radial/ulnar deviation.

It was not until 1995 that Craigen and Stanley (18) published a paper that questioned the validity of both the row and the column theories. They proposed that actual carpal motion involved some combination of the two theories, or perhaps something altogether more complex. Since that time, numerous studies have shown that carpal motion is far more complicated than either the column or the row theories. To date, there is no unifying theory of carpal motion.

1.2.3 The Dart Throwing Motion

The Dart Throwing Motion has been described as the most important functional wrist motion (19). Traditionally, kinematic studies of the wrist have been focused on the orthogonal flexion/extension and radial/ulnar deviation motions (**Figure 1.4**). During wrist flexion/extension, the scaphoid and lunate flex and extend with the wrist. During wrist radial/ulnar deviation, both bones continue to rotate in the flexion/extension plane; flexing during wrist radial deviation and extending during wrist ulnar deviation (20-24). In 1985, Palmer et al. measured wrist motion during tasks of daily living and was able to show that a great many tasks involve a motion from radial extension to ulnar flexion, which they described as the Dart Thrower's Motion (2). Since then, it has been shown that the scaphoid and lunate rotate less during the DTM than during pure flexion/extension or radial/ulnar deviation (25-27). The DTM has been hypothesized to have played a role in human evolution (28). Used in activities such as throwing rocks, wielding a club, throwing a spear and hammering, the DTM has been shown to be the

direction in which the wrist has its greatest overall range of motion (3). Despite the importance of the DTM, relatively few studies have targeted this motion.

1.2.4 Total Wrist Arthroplasty

Our limited understanding of wrist function has resulted in few choices for patients with advanced wrist disease. Arthroplasty has achieved considerable success in other joints in the body. However, there remains a preference for treating advanced cases of osteoarthritis in the wrist with some type of arthrodesis instead of a total wrist arthroplasty (TWA). This preference exists in spite of the fact that most arthrodeses limit range of motion by almost 50% relative to the non-surgical wrist, and in the most extreme case, a total wrist arthrodesis eliminates all wrist motion (29). Despite more than 40 years of experience with TWA (30), the current generation of wrist implants still fails to replace arthrodesis. Ironically, the TWA is recommended for lower demand patients. These patients are specifically restricted from common activities that include regularly lifting more than 10lbs. For those that choose a TWA, there continues to be complications associated with higher rates of failure and revision as compared to arthrodesis (31).

A major limitation with the current generation of TWA is their ellipsoidal designs, which are based on two independent directions of wrist motion: flexion/extension and radial/ulnar deviation. This design results from a long history of measuring and reporting wrist motion in these two directions. However, alternative directions of wrist motion, such as the DTM, are thought to be more physiologically relevant. By studying the wrist under more functional and loaded conditions, we hope to

gain greater insight into its behavior. This knowledge could be incorporated into the next generation of wrist implants, such that they might be better able to mimic the function of the normal human carpus. A new generation of artificial wrists designed to rotate about a physiologic axis instead of the historic orthogonal axes could achieve results that surpass arthrodesis, and improve the quality of life for these patients.

1.2.5 Markerless Bone Registration

Markerless Bone Registration (MBR) is an established method for accurately measuring *in vivo* carpal kinematics without invasive pins or markers (32-38). There are significant challenges in accurately studying the kinematics of the wrist. The small size of the carpus and the complex 3-D motions of each bone make it incredibly difficult to investigate. External surface markers cannot track the motion of individual carpal bones, only overall wrist motion. Studies of carpal kinematics using more invasive markers pose greater challenges and risk affecting the carpal kinematics of interest.

Based on serial static CT scans, MBR provides a semi-automated method for *in vivo* measurements of carpal kinematics. Briefly, the cortical shell of each bone is manually segmented using Mimics 9.11 (Materialise, Leuven, Belgium) to produce 3-D bone models. Custom C++ code (GNU gcc, Free Software Foundation, Boston, Massachusetts) is used to track the segmented bones in subsequent scans. Additional custom Matlab code (Matlab 2007b, The MathWorks, Natick, Massachusetts) is used to register the radii together and eliminate small motions of the forearm between scans.

The accuracy of this methodology has been established as better than 0.5mm in translation and 1° in rotation using a 0.97mm x 0.97mm x 1mm volume set. This

accuracy is improved by almost 50% when using a 0.3mm x 0.3mm x 1mm volume (38, 39). With our planned image resolution of at least 0.6mm x 0.6mm x 0.6mm volume set, our kinematic accuracy should be better than 0.5mm of translational error and 1° rotational error. In addition to carpal kinematics, this method has been shown effective at measuring the kinematics of the distal radioulnar joint (DRUJ) (40).

1.3 Carpal and Forearm Kinematics During a Simulated Hammering Task

1.3.1 Hammering

Hammering is a forceful occupational task accomplished via extension of the shoulder and elbow and use of the DTM at the wrist. Wrist motion during hammering has been measured using external markers in two different studies. Palmer et al. was able to show that hammering uses the DTM and occurs almost entirely in extension (2). Schoenmarklin et al. measured the effects of handle angle on wrist motion and performance during hammering (41). Wrist motion was tracked using an external “wrist monitor” that was attached to the distal forearm and tracked the motion of the 2nd and 4th proximal phalanges. While they found that both hammer handle angle and the type of hammering affected the range of motion as well as the ratio of flexion/extension to radial/ulnar deviation, all hammering took place in extension and followed a DTM-like path. However, both of these studies used external tracking devices, which prevented them from measuring the motion of individual carpal bones.

While the kinematics of the carpus during the DTM has been measured *in vitro* (26, 27), only one study has specifically targeted the DTM *in vivo*. Moritomo et al. measured carpal motion *in vivo* during a DTM using an MRI-based markerless bone-registration technique (42). The subjects in this study had their wrists imaged at 6 targeted positions from 60° of radial extension to 40° of ulnar flexion. These wrist positions followed the DTM from radial extension to ulnar flexion and the rotation of the

scaphoid and lunate were both reduced. However, this path of wrist motion was most likely *not* the path associated with hammering. Prior *in vivo* hammering studies (2, 41) have established that hammering takes place almost entirely in extension, while Moritomo et al. appear to have targeted a path of wrist motion almost evenly divided between extension and flexion. Based on this information, it appears that they measured kinematics in a path parallel to hammering, but still distinct from the true hammering path. Our study was unique, in that it was the first time carpal kinematics were measured during a functional task.

1.3.2 Static vs. Dynamic Hammering

Static hammering can be used to simulate dynamic hammering. Curran et al. found that wrist motion during static and dynamic hammering followed similar paths (43). They measured the kinematics of the wrist relative to the forearm using MTx Inertial Measurement Units (IMU) (Xsens Technologies B.V., The Netherlands) in 11 healthy male volunteers. Based on these results, we feel confident that results obtained during a simulated hammering study can be applied to dynamic hammering.

1.3.3 Relevance

In vivo measurements of carpal motion during functional tasks are critical to our understanding of carpal function. This understanding is relevant for both basic scientists and clinicians. Improved knowledge of carpal kinematics during functional tasks that utilize the DTM could impact what treatments clinicians choose for their patients. Because rotation at the radiocarpal joint is minimized during the DTM, it has been

suggested that a radio-scapho-lunate fusion could be more appropriate for patients with arthritis at the radiocarpal joint (19). Rehabilitation protocols could also be affected by our understanding of carpal kinematics. By allowing limited motion along the DTM, it might possible to introduce early rehabilitation to the wrist while minimizing motion at an injured radiocarpal joint.

1.4 Conformational Changes in the Carpus During Finger Traps Distraction

1.4.1 Carpal Loading

A complete understanding of the wrist is dependent upon understanding not only how the unloaded wrist moves, but also how it handles loads. Under normal conditions, the healthy wrist is subjected to both compressive and tensile loads. To date, most research on the carpus under load has been focused on radiocarpal joint contact area and pressure distribution using a variety of invasive techniques.

Earlier work was performed primarily *in vitro* using FujiFilm to measure the contact center and contact area of the radioscaphoid and radiolunate joints. These authors found that joint contact area was limited to only 20% of the overall joint surface in both joints. The ratio of scaphoid contact area to lunate contact area was on average 1.47 (44, 45). Two groups developed their own custom sensors to measure joint contact pressures and areas, using sensors that were 1mm and 1.6mm thick, respectively (46, 47). Hara et al. (47) established that 15% of load was carried by the ulna and 85% by the radius, of which almost 2/3 was from the scaphoid and 1/3 from the lunate. Rikli et al. (46) only measured a single *in vivo* wrist and found an almost even distribution of load between the radius and the ulna. It is unknown what effect inserting a 1mm or 1.6mm thick sensor has on the forces being recorded. The effect of compressive loading on carpal motion has only been examined in a single study. Kobayashi et al. (48) applied an axial load of 98N to 13 cadaver wrists with the wrist fixed in the neutral position. They found that

compressive loading caused the scaphoid and lunate to rotate on average 5.1° and 4.2° , respectively.

Simulated distraction in a cadaver model demonstrated that 4mm of distraction across the carpus could be achieved using 20N (2kg) of load, and 8mm of distraction was achieved using 80N (8kg) of load (49). This model was limited by the fact that overall motion was restricted to a single degree of freedom (distraction), and no attempt was made to reproduce normal muscle tone. Further, carpal measurements were recorded for only a few bones and these measurements were made using anteroposterior radiographs limiting analysis to only two-dimensions.

The three-dimensional effects of a tensive load were only measured in a single cadaveric study (26) where the authors demonstrated that distraction reduced radiocarpal motion during extension and increased radiocarpal motion during flexion. The effect of load on the wrist independent of motion was not recorded, nor have these findings been confirmed *in vivo*. Due to the paucity of information on the effect of distraction on the carpus in the literature, we chose to focus our study of carpal loading on a tensive task. There is additional immediate clinical relevance because wrist distraction is used during surgery, as well as in the treatment of a variety of wrist injuries.

1.4.2 Clinical Relevance

Distraction can be beneficial by reducing load on articular cartilage or across a fracture site and is used in the treatment of distal radius fractures (50). While studies have shown that distraction is associated with a decline in outcome measures (51, 52), it

is difficult to interpret and apply those findings without first understanding how distraction affects the wrist.

Distraction has been used in the diagnosis of scapholunate ligament injury. In this “carpal stress test” (53), a posteroanterior radiograph of the wrist under traction was used in the diagnosis of ligament injury. A visible stepoff at the scapholunate joint was considered indicative of injury. A similar test showed that under traction, patients with scapholunate ligament tears exhibited widening of the scapholunate distance by 1mm or more (54). While both of these studies were able to show significant differences between the uninjured and injured wrists, an earlier study using similar techniques found sensitivity and specificity were variable, thus concluding that such testing was not useful for the diagnosis of chronic wrist pain (55). Unfortunately, all of these studies measured changes of a limited number of carpal bones, and changes were examined in only two dimensions under posteroanterior radiographs.

1.4.3 Computer Models

Computer models have been used to estimate force transmission through the wrist in both 2-D and 3-D using a variety of methods (13, 56, 57). While these computational models are impressive, they are almost entirely based on a single bone model of the unloaded wrist. Without a second position to measure changes from the first position, it is incredibly difficult to develop and test such models. Only two studies have used multiple positions of the same wrist in their models. The first study estimated *in vivo* cartilage contact area and pressures at the radiocarpal joint before and after gripping a cylinder (58). There are a number of shortcomings to this study; these shortcomings

include the use of an untested kinematic tracking method and various gross assumptions, such as assuming all cartilage to be uniformly 1mm thick. The second study used wrists in a single unloaded neutral position and a second loaded extension position (59). However, with such a large change in wrist posture (almost 90°), it is difficult to differentiate between the effect of loading and the effect of extending the wrist. The development of accurate computer models would be aided by *in vivo* data of the same wrist before and after loading. Such information could be used to train and to validate such models.

1.5 Specific Aims

Specific Aim 1 – Determine the kinematics of the wrist and forearm during simulated hammering.

The objectives of the first aim were to examine the full three-dimensional (3-D) motion of the bones in the wrist and the pronation/supination of the forearm during simulated hammering, and to determine the *in vivo* 3-D carpal kinematics during this important functional task. Hammering is a dominant task in which the wrist moves from a position of radial extension to ulnar flexion at the tail end of an overall motion that also involves shoulder and elbow extension (41). The overall motion of the wrist from radial extension to ulnar flexion has been described as the Dart Thrower's Motion (DTM). Previous studies have shown that rotation of the scaphoid and lunate are minimized during the DTM (25, 27, 42); however, this observation has never been confirmed *in vivo* during a functional task. Understanding the kinematics of the carpus during functional tasks can be applied towards design of ergonomic tools as well as designing rehabilitation protocols to isolate the midcarpal joint while minimizing motion at the radiocarpal joint.

Specific Aim 2 – Measure the change in carpal kinematics during distractive loading of the wrist.

The objective of the second aim was to observe the effect of a tensive distractive load on the carpus. Most studies involving tensive loads in the carpus have been performed on cadavers (26, 60, 61). To date, no one has measured how these loads affect the spacing of the carpus *in vivo*. By using an *in vivo* model, we have eliminated the enormous complexity associated with trying to replicate the appropriate muscle tone and loading that is used to balance the wrist in cadaveric studies. Knowledge of how the wrist reacts to these loads is important if we wish to completely understand how the wrist functions. Such knowledge could be applied towards designing computer models of the wrist and understanding the mechanical properties of the carpal ligaments. Additionally, wrist function under tension has direct clinical applicability. This work could help us to determine why patients respond differently to traction, which is used for a variety of procedures.

1.6 References

1. Dillon, C., Petersen, M., and Tanaka, S., *Self-reported hand and wrist arthritis and occupation: data from the U.S. National Health Interview Survey-Occupational Health Supplement*. Am J Ind Med, 2002. **42**(4): 318-327.
2. Palmer, A.K., Werner, F.W., Murphy, D., and Glisson, R., *Functional wrist motion: a biomechanical study*. J Hand Surg [Am], 1985. **10**(1): 39-46.
3. Li, Z.M., Kuxhaus, L., Fisk, J.A., and Christophel, T.H., *Coupling between wrist flexion-extension and radial-ulnar deviation*. Clin Biomech (Bristol, Avon), 2005. **20**(2): 177-183.
4. Ryu, J.Y., Cooney, W.P., 3rd, Askew, L.J., An, K.N., and Chao, E.Y., *Functional ranges of motion of the wrist joint*. J Hand Surg [Am], 1991. **16**(3): 409-419.
5. Crisco, J.J., Pike, S., Hulsizer-Galvin, D.L., Akelman, E., Weiss, A.P., and Wolfe, S.W., *Carpal bone postures and motions are abnormal in both wrists of patients with unilateral scapholunate interosseous ligament tears*. J Hand Surg [Am], 2003. **28**(6): 926-937.
6. Leventhal, E.L., Wolfe, S.W., Moore, D.C., Akelman, E., Weiss, A.P., and Crisco, J.J., *Interfragmentary motion in patients with scaphoid nonunion*. J Hand Surg [Am], 2008. **33**(7): 1108-1115.
7. Short, W.H., Werner, F.W., Green, J.K., Weiner, M.M., and Masaoka, S., *The effect of sectioning the dorsal radiocarpal ligament and insertion of a pressure sensor into the radiocarpal joint on scaphoid and lunate kinematics*. J Hand Surg [Am], 2002. **27**(1): 68-76.
8. Vender, M.I., Watson, H.K., Wiener, B.D., and Black, D.M., *Degenerative change in symptomatic scaphoid nonunion*. J Hand Surg [Am], 1987. **12**(4): 514-519.
9. Watson, H.K. and Ballet, F.L., *The SLAC wrist: scapholunate advanced collapse pattern of degenerative arthritis*. J Hand Surg [Am], 1984. **9**(3): 358-365.
10. Mack, G.R., Bosse, M.J., Gelberman, R.H., and Yu, E., *The natural history of scaphoid non-union*. J Bone Joint Surg Am, 1984. **66**(4): 504-509.
11. Watson, H.K. and Brenner, L.H., *Degenerative disorders of the wrist*. J Hand Surg [Am], 1985. **10**(6 Pt 2): 1002-1006.
12. Watson, H.K., Weinzwieg, J., and Zeppieri, J., *The natural progression of scaphoid instability*. Hand Clin, 1997. **13**(1): 39-49.
13. Iwasaki, N., Genda, E., Minami, A., Kaneda, K., and Chao, E.Y., *Force transmission through the wrist joint in Kienbock's disease: a two-dimensional theoretical study*. J Hand Surg [Am], 1998. **23**(3): 415-424.
14. Schuind, F., Eslami, S., and Ledoux, P., *Kienbock's disease*. J Bone Joint Surg Br, 2008. **90**(2): 133-139.
15. Bryce, T.H., *Certain Points in the Anatomy and Mechanism of the Wrist-Joint Reviewed in the Light of a Series of Rontgen Ray Photographs of the Living Hand*. J Anat Physiol, 1896. **31**(Pt 1): 59-79.
16. Navarro, A., *Luxaciones del carpo*. Anales de la Facultad de Medicina, 1921. **6**: 113-141.
17. Taleisnik, J., *The ligaments of the wrist*. J Hand Surg [Am], 1976. **1**(2): 110-118.

18. Craigie, M.A. and Stanley, J.K., *Wrist kinematics. Row, column or both?* J Hand Surg [Br], 1995. **20**(2): 165-170.
19. Moritomo, H., Apergis, E.P., Herzberg, G., Werner, F.W., Wolfe, S.W., and Garcia-Elias, M., *2007 IFSSH committee report of wrist biomechanics committee: biomechanics of the so-called dart-throwing motion of the wrist.* J Hand Surg [Am], 2007. **32**(9): 1447-1453.
20. Moojen, T.M., Snel, J.G., Ritt, M.J., Kauer, J.M., Venema, H.W., and Bos, K.E., *Three-dimensional carpal kinematics in vivo.* Clin Biomech (Bristol, Avon), 2002. **17**(7): 506-514.
21. Short, W.H., Werner, F.W., Fortino, M.D., and Mann, K.A., *Analysis of the kinematics of the scaphoid and lunate in the intact wrist joint.* Hand Clin, 1997. **13**(1): 93-108.
22. Wolfe, S.W., Neu, C., and Crisco, J.J., *In vivo scaphoid, lunate, and capitate kinematics in flexion and in extension.* J Hand Surg [Am], 2000. **25**(5): 860-869.
23. Fick, *Handbuch der Anatomie und Mechanik der Gelenke.* Vol. Part 3. 1911: Fischer, Jena. 657-659.
24. Patterson, R.M., Nicodemus, C.L., Viegas, S.F., Elder, K.W., and Rosenblatt, J., *High-speed, three-dimensional kinematic analysis of the normal wrist.* J Hand Surg [Am], 1998. **23**(3): 446-453.
25. Crisco, J.J., Coburn, J.C., Moore, D.C., Akelman, E., Weiss, A.P., and Wolfe, S.W., *In vivo radiocarpal kinematics and the dart thrower's motion.* J Bone Joint Surg Am, 2005. **87**(12): 2729-2740.
26. Ishikawa, J., Cooney, W.P., 3rd, Niebur, G., An, K.N., Minami, A., and Kaneda, K., *The effects of wrist distraction on carpal kinematics.* J Hand Surg [Am], 1999. **24**(1): 113-120.
27. Werner, F.W., Green, J.K., Short, W.H., and Masaoka, S., *Scaphoid and lunate motion during a wrist dart throw motion.* J Hand Surg [Am], 2004. **29**(3): 418-422.
28. Wolfe, S.W., Crisco, J.J., Orr, C.M., and Marzke, M.W., *The dart-throwing motion of the wrist: is it unique to humans?* J Hand Surg [Am], 2006. **31**(9): 1429-1437.
29. Weiss, K.E. and Rodner, C.M., *Osteoarthritis of the wrist.* J Hand Surg [Am], 2007. **32**(5): 725-746.
30. Carlson, J.R. and Simmons, B.P., *Total wrist arthroplasty.* J Am Acad Orthop Surg, 1998. **6**(5): 308-315.
31. Cavaliere, C.M. and Chung, K.C., *A systematic review of total wrist arthroplasty compared with total wrist arthrodesis for rheumatoid arthritis.* Plast Reconstr Surg, 2008. **122**(3): 813-825.
32. Crisco, J.J. and McGovern, R.D., *Efficient calculation of mass moments of inertia for segmented homogeneous three-dimensional objects.* J Biomech, 1998. **31**(1): 97-101.
33. Crisco, J.J., McGovern, R.D., and Wolfe, S.W., *Noninvasive technique for measuring in vivo three-dimensional carpal bone kinematics.* J Orthop Res, 1999. **17**(1): 96-100.

34. Crisco, J.J., Wolfe, S.W., Neu, C.P., and Pike, S., *Advances in the in vivo measurement of normal and abnormal carpal kinematics*. Orthop Clin North Am, 2001. **32**(2): 219-231, vii.
35. Wolfe, S.W., Crisco, J.J., and Katz, L.D., *A non-invasive method for studying in vivo carpal kinematics*. J Hand Surg [Br], 1997. **22**(2): 147-152.
36. Marai, G.E., Crisco, J.J., and Laidlaw, D.H., *A kinematics-based method for generating cartilage maps and deformations in the multi-articulating wrist joint from CT images*. Conf Proc IEEE Eng Med Biol Soc, 2006. **1**: 2079-2082.
37. Marai, G.E., Laidlaw, D.H., Coburn, J.C., Upal, M.A., and Crisco, J.J. *A 3D Method for Segmenting and Registering Carpal Bones from CT Volume Images*. in *Annual Meeting of the American Society of Biomechanics*. 2003. Toledo, OH.
38. Marai, G.E., Laidlaw, D.H., and Crisco, J.J., *Super-resolution registration using tissue-classified distance fields*. IEEE Trans Med Imaging, 2006. **25**(2): 177-187.
39. Neu, C.P., McGovern, R.D., and Crisco, J.J., *Kinematic accuracy of three surface registration methods in a three-dimensional wrist bone study*. J Biomech Eng, 2000. **122**(5): 528-533.
40. Moore, D.C., Hogan, K.A., Crisco, J.J., 3rd, Akelman, E., Dasilva, M.F., and Weiss, A.P., *Three-dimensional in vivo kinematics of the distal radioulnar joint in malunited distal radius fractures*. J Hand Surg [Am], 2002. **27**(2): 233-242.
41. Schoenmarklin, R.W. and Marras, W.S., *Effects of handle angle and work orientation on hammering: I. Wrist motion and hammering performance*. Hum Factors, 1989. **31**(4): 397-411.
42. Moritomo, H., Murase, T., Goto, A., Oka, K., Sugamoto, K., and Yoshikawa, H., *In vivo three-dimensional kinematics of the midcarpal joint of the wrist*. J Bone Joint Surg Am, 2006. **88**(3): 611-621.
43. Curan, P.F., Rainbow, M.J., Moore, D.C., and Crisco, J.J. *Hammering and Dart Throwing are Kinematically Different*. in *American Society of Biomechanics*. 2007. Stanford University, Stanford, CA.
44. Viegas, S.F., Tencer, A.F., Cantrell, J., Chang, M., Clegg, P., Hicks, C., O'Meara, C., and Williamson, J.B., *Load transfer characteristics of the wrist. Part I. The normal joint*. J Hand Surg [Am], 1987. **12**(6): 971-978.
45. Kazuki, K., Kusunoki, M., and Shimazu, A., *Pressure distribution in the radiocarpal joint measured with a densitometer designed for pressure-sensitive film*. J Hand Surg [Am], 1991. **16**(3): 401-408.
46. Rikli, D.A., Honigmann, P., Babst, R., Cristalli, A., Morlock, M.M., and Mittlmeier, T., *Intra-articular pressure measurement in the radioulnocarpal joint using a novel sensor: in vitro and in vivo results*. J Hand Surg [Am], 2007. **32**(1): 67-75.
47. Hara, T., Horii, E., An, K.N., Cooney, W.P., Linscheid, R.L., and Chao, E.Y., *Force distribution across wrist joint: application of pressure-sensitive conductive rubber*. J Hand Surg [Am], 1992. **17**(2): 339-347.
48. Kobayashi, M., Garcia-Elias, M., Nagy, L., Ritt, M.J., An, K.N., Cooney, W.P., and Linscheid, R.L., *Axial loading induces rotation of the proximal carpal row bones around unique screw-displacement axes*. J Biomech, 1997. **30**(11-12): 1165-1167.

49. Loebig, T.G., Badia, A., Anderson, D.D., and Baratz, M.E., *Correlation of wrist ligamentotaxis with carpal distraction: implications for external fixation*. J Hand Surg [Am], 1997. **22**(6): 1052-1056.
50. Fernandez, D.L. and Mader, K., *The treatment of complex carpal dislocations by external fixation*. Injury, 2000. **31 Suppl 1**: 92-101.
51. Kaempffe, F.A., *External fixation for distal radius fractures: adverse effects of excess distraction*. Am J Orthop, 1996. **25**(3): 205-209.
52. Kaempffe, F.A. and Walker, K.M., *External fixation for distal radius fractures: effect of distraction on outcome*. Clin Orthop Relat Res, 2000(380): 220-225.
53. Yamaguchi, S., Beppu, M., Matsushita, K., and Takahashi, K., *The carpal stretch test at the scapholunate joint*. J Hand Surg [Am], 1998. **23**(4): 617-625.
54. Schadel-Hopfner, M., Bohringer, G., Gotzen, L., and Celik, I., *Traction radiography for the diagnosis of scapholunate ligament tears*. J Hand Surg [Br], 2005. **30**(5): 464-467.
55. Fortems, Y., Mawhinney, I., Lawrence, T., and Stanley, J.K., *Traction radiographs in the diagnosis of chronic wrist pain*. J Hand Surg [Br], 1994. **19**(3): 334-337.
56. Schuind, F., Cooney, W.P., Linscheid, R.L., An, K.N., and Chao, E.Y., *Force and pressure transmission through the normal wrist. A theoretical two-dimensional study in the posteroanterior plane*. J Biomech, 1995. **28**(5): 587-601.
57. Carrigan, S.D., Whiteside, R.A., Pichora, D.R., and Small, C.F., *Development of a three-dimensional finite element model for carpal load transmission in a static neutral posture*. Ann Biomed Eng, 2003. **31**(6): 718-725.
58. Pillai, R.R., Thoomukuntla, B., Ateshian, G.A., and Fischer, K.J., *MRI-based modeling for evaluation of in vivo contact mechanics in the human wrist during active light grasp*. J Biomech, 2007. **40**(12): 2781-2787.
59. Majima, M., Horii, E., Matsuki, H., Hirata, H., and Genda, E., *Load transmission through the wrist in the extended position*. J Hand Surg [Am], 2008. **33**(2): 182-188.
60. Cho, M.S., Means, K.R., Shrout, J.A., and Segalman, K.A., *Carpal tunnel volume changes of the wrist under distraction*. J Hand Surg Eur Vol, 2008. **33**(5): 648-652.
61. Baechler, M.F., Means, K.R., Jr., Parks, B.G., Nguyen, A., and Segalman, K.A., *Carpal canal pressure of the distracted wrist*. J Hand Surg [Am], 2004. **29**(5): 858-864.

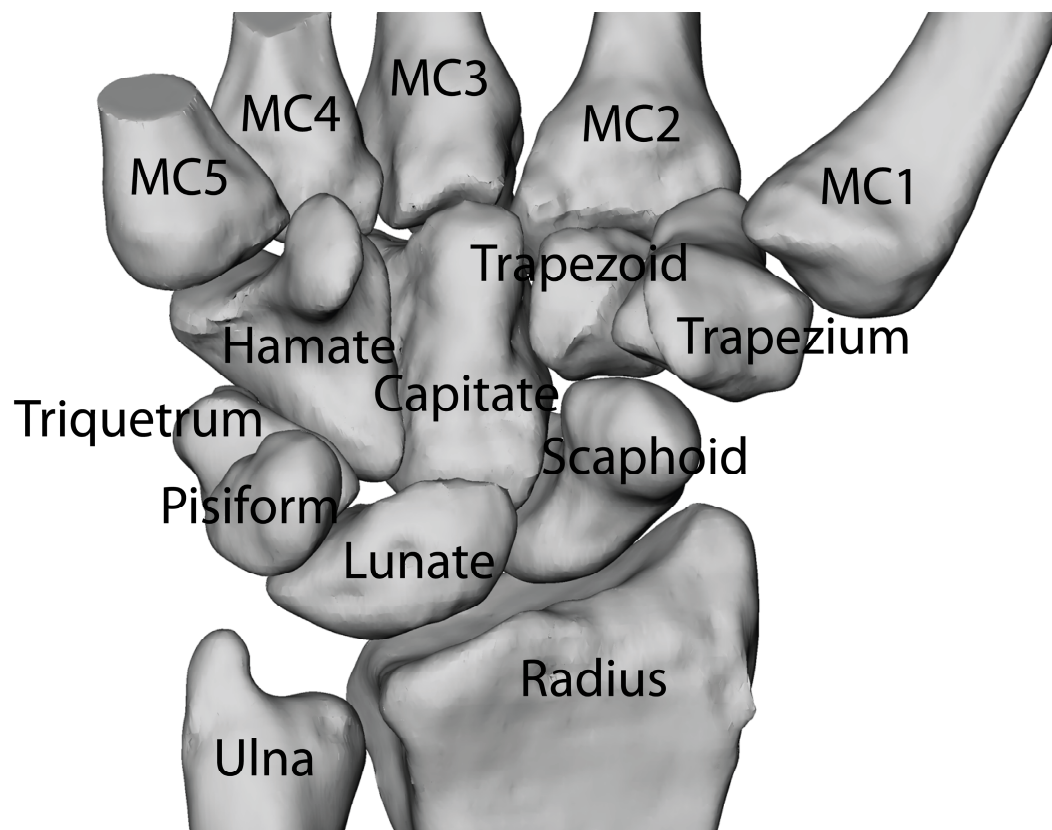


Figure 1.1. Volar view of a right wrist (MC = Metacarpal).

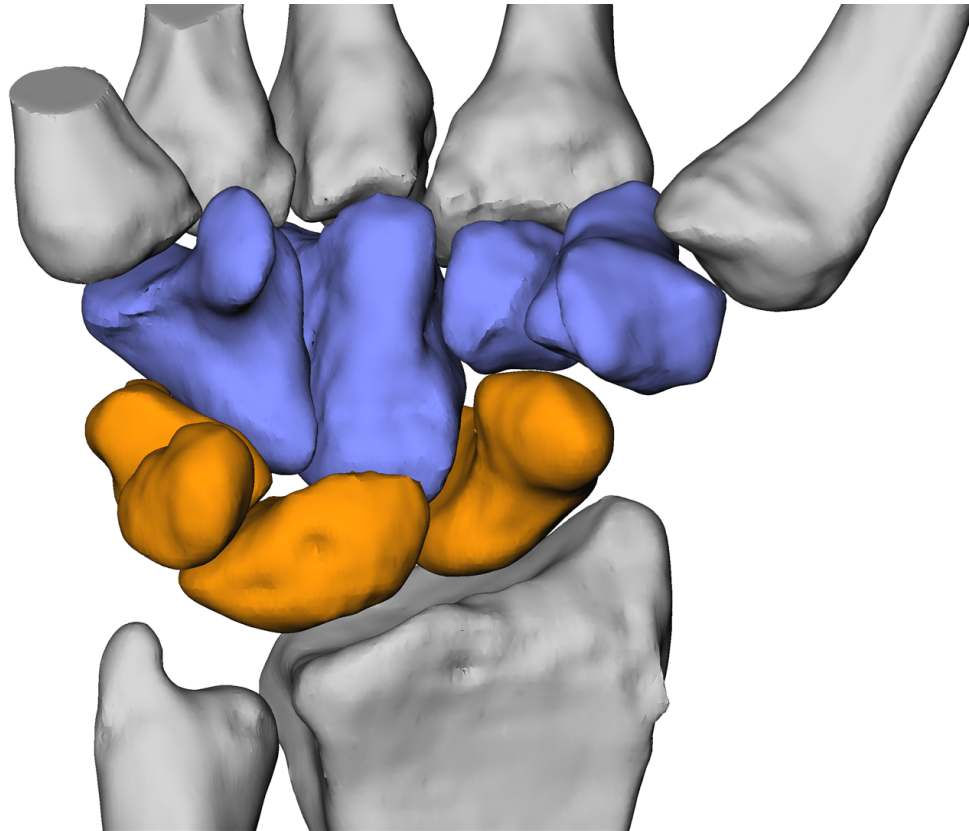


Figure 1.2. Volar view of a right wrist highlighting the proximal row (scaphoid, lunate, triquetrum and pisiform) in orange and the distal row (trapezium, trapezoid, capitate and hamate) in blue.

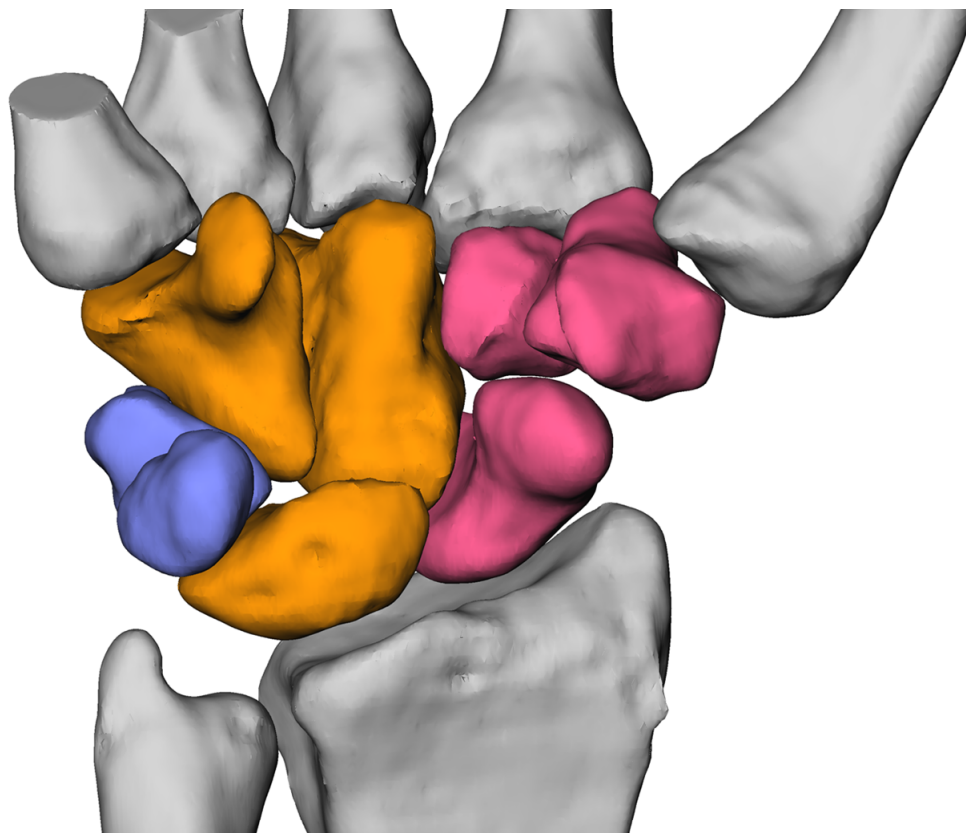
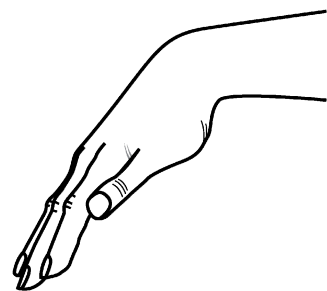
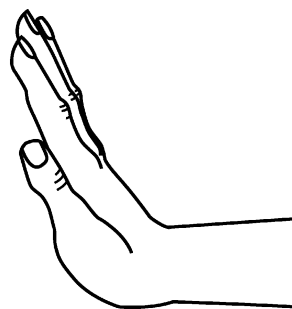


Figure 1.3. Volar view of a right wrist highlighting the three columns in the original columnar theory as proposed by Navarro (ref). In this model, the central column is composed of the lunate, capitate and hamate (orange); the medial column is composed of the triquetrum and pisiform (blue); and the lateral column is composed of the scaphoid, trapezium and trapezoid (magenta).



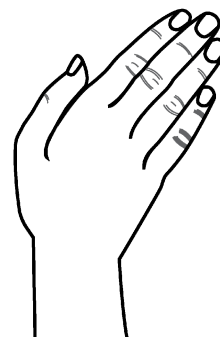
Flexion



Extension



Radial
Deviation



Ulnar
Deviation

Figure 1.4. Wrist position is conventionally described in two orthogonal directions: flexion/extension and radial/ulnar deviation.

Chapter 2

Carpal and Forearm Kinematics During a Simulated Hammering Task

Evan L. Leventhal, Douglas C. Moore, Edward Akelman, Scott W. Wolfe
and Joseph J. Crisco

The following chapter is in preparation for submission to the *Journal of Hand Surgery*.

2.1 Abstract

2.1.1 Introduction

Hammering is a forceful task thought to use the Dart Throwing Motion (DTM) at the wrist. The purpose of this study was to measure the actual path of wrist and forearm motion used during hammering by live subjects, as well as the kinematics of the scaphoid and lunate. We hypothesized that hammering uses a DTM and that there would be zero radiocarpal motion during this task.

2.1.2 Methods

13 healthy volunteers consented to have their dominant wrist and distal forearm imaged with computed tomography at five positions in a simulated hammering task. The kinematics of the carpus and distal radial ulnar joint were measured using markerless bone registration. The direction of wrist motion was described as the angle between the path of wrist motion and the sagittal plane. In addition, forearm rotation, radioscaphoid and radiolunate motion were computed as a function of wrist position.

2.1.3 Results

All volunteers performed the simulated hammering task using a path of wrist motion from radial extension to ulnar flexion (DTM) that was offset in an extended position. The average path of wrist motion was oriented 41° from the sagittal plane. During this motion, rotations of the scaphoid and lunate averaged 40% and 41% respectively of total wrist motion. Range of forearm pronation/supination averaged only $12 \pm 8^\circ$ during hammering.

2.1.4 Conclusions

Wrist motion during the simulated path followed a DTM, but in an offset extended position. Radiocarpal motion was not minimized which may reflect a limitation of simulating hammering with static postures, although scaphoid and lunate rotation were significantly reduced when compared with rotations during pure wrist flexion/extension.

2.2 Introduction

During hammering, the wrist moves from a position of radial extension to ulnar flexion at the tail end of an overall motion that also involves shoulder extension and elbow extension (1). Pronation and supination of the forearm during hammering have never been reported, although it has been hypothesized that the forearm naturally pronates during radial extension and supinates during ulnar flexion (2). The overall motion of the wrist from radial extension to ulnar flexion has been described as the Dart Thrower's Motion (DTM). Hammering is just one of many activities of daily living that utilize this wrist motion (3), which has been described as the most important functional wrist motion (3). Understanding how the wrist functions during hammering and other DTM-related tasks has important implications for the design of ergonomic tools, rehabilitation protocols, and wrist implants.

Most of what is known about hammering has been learned from data collected using electro-mechanical devices attached to the distal forearm and hand. These studies suggest that hammering takes place with the wrist primarily in extension and that it generally follows a DTM-like path (1, 4). However, externally applied tracking devices are incapable of yielding data regarding the motion of the individual carpal bones. Additionally, because the systems used in these studies only had sensors attached to the distal forearm and hand, they could not provide data on forearm pronation/supination.

The kinematics of the carpus during the DTM has been studied in cadaver experiments and in living subjects (5-9). While all of these studies have reported decreased radiocarpal motion during the DTM compared to pure flexion and extension of

the wrist, their data regarding the relative contribution of radiocarpal motion to overall wrist motion have varied. In particular, scaphoid rotation during the DTM has been reported to be as low as 26% and as high as 50% of wrist motion (5-9), while lunate rotation has similarly been reported to range between 22% and 40% of wrist motion (5-9). Analyzing *in vivo* carpal kinematics from 504 wrist positions from 28 subjects, Crisco et al. (8) found that scaphoid and lunate rotations approaches zero along paths of the DTM.

While carpal kinematics during the DTM has been studied extensively with various wrist motion protocols, to this point there is no data on functional carpal kinematics during high-demand functional tasks such as hammering. In addition, the degree to which forearm pronation/supination contributes to hammering is unknown. The purpose of this study was to examine the full three-dimensional (3-D) motion of the bones in the wrist and the pronation/supination of the forearm during hammering and to determine the *in vivo* 3-D carpal kinematics during this important functional task. We hypothesized that wrist motion would follow the dart thrower's path and that there would be zero radiocarpal motion during this hammering task.

2.3 Methods

2.3.1 Volunteer Selection and CT Scanning

With IRB approval, 13 healthy, right hand dominant volunteers (6 male, 7 female; average age 24.8, range [21-31]) were recruited. Each volunteer was screened and excluded from the study if there was a prior history of wrist disease, injury, or any soft tissue or metabolic disease that could affect carpal motion (i.e. severe osteoporosis, hyperthyroidism). All volunteers were relative novices at hammering, primarily composed of students and young professionals.

The dominant wrist of each volunteer was scanned in 5 positions along the hammering path. During scanning, their forearms and hands were steadied with the use of a custom-designed jig that included a wrist rest and as well as stops for the hammer handle at each of the 5 positions. Stop were located at: -40° (windup), -20° , 0° (neutral, hammer handle orthogonal to forearm), 20° , and 40° (impact) (**Figure 2.1**). Subjects were positioned prone on the CT table with their chest supported. The right arm was extended from the torso and at neutral abduction, parallel with the scanning table. At each of the five hammering positions a single CT scan was acquired of the dominant wrist. A sixth, higher resolution CT scan was acquired of the wrist in a neutral position for segmentation purposes. Scanning was performed at 80kVp and 80mA, with at least 0.5mm x 0.5mm in plane resolution and slice thickness of 0.6mm using a GE LightSpeed 16 (General Electric, Milwaukee, WI).

2.3.2 Kinematic Analysis

The 3-D kinematics of each carpal bone, as well as the radius, ulna and the metacarpal bones were calculated using our established CT-based markerless bone registration methodology (10). Briefly, each bone was manually segmented from the high resolution neutral scan using Mimics 9.11 (Materialise, Leuven, Belgium). Custom C++ (GNU gcc, Free Software Foundation, Boston, Massachusetts) and Matlab (The MathWorks, Natick, Massachusetts) code was then used to calculate the position of each forearm, carpal and metacarpal bone in the five CT volume images of hammering. As part of these calculations, the radius of each forearm was aligned in each of the image sets to account for possible movement of the forearm between scans. Wrist position was defined by the orientation of the inertially defined long axis of the third metacarpal (11) with respect to a standard radius-based coordinate system (12). Motion of the scaphoid and lunate with respect to the radius (radioscaphoid and radiolunate motion) were described using Helical Axes of Motion (HAM) variables. Rotation of the scaphoid and lunate were computed using the neutral hammering position as the starting position.

2.3.3 Pronation/Supination Kinematics

Forearm pronation/supination rotation during the hammering task was estimated by measuring the rotation of the radius relative to the ulnar at each position from the starting neutral hammering position. The neutral forearm pronation/supination position was computed based on the orientation of the radius relative to the humerus when the elbow was flexed at 90°. Our scans did not include the humerus, so the orientation of the humerus was estimated using the orientation of the distal ulnar. The normal relationship between the orientation of the humerus and the distal ulnar when the elbow

was flexed at 90° was determined in a 7 cadaver pilot study. Specifically, the average orientation of an ulnar-based coordinate system (x-axis directed along the long axis of the distal ulnar, y-axis directed towards the ulnar styloid, orthogonal to the x-axis, and the z-axis orthogonal to the x and y-axes) (12) relative to the humoral long axis was computed. The average angle between the y-axis of this coordinate system (corresponding to the direction of the ulnar styloid) and the humoral long axis was determined to be $172 \pm 10^\circ$.

Neutral pronation/supination was therefore defined as the position where the flexion/extension axis of the previously defined radius-based coordinate system was oriented 172° from the ulnar coordinate system. This corresponded to the clinical definition of neutral forearm pronation/supination (with the thumb extended, wrist in neutral and the elbow at 90° of flexion, the thumb is parallel to the humerus when in neutral forearm rotation).

2.3.4 Data Analysis

Wrist range of motion during hammering was calculated for each subject as the difference in wrist position at the full windup (-40°) and the full impact (-40°) positions. Similarly, forearm pronation/supination range of motion was calculated for each subject as the difference in forearm pronation/supination position between the full windup and full impact hammering positions.

Because the wrist motion involved a combination of flexion/extension and radial/ulnar deviation, the direction of wrist motion was described in terms of a “coupling ratio” (13), or the ratio of flexion/extension to radial/ulnar deviation. (e.g. pure flexion/extension = 0, equal parts flexion/extension and radial/ulnar deviation = 1, pure

radial/ulnar deviation = ∞) Direction of wrist motion was also described in terms of the path of motion reflected onto a plane perpendicular to the long axis of the radius (i.e. the yz-plane of the radial coordinate system). The direction of motion was then described as the angle of the reflected path with respect to the z-axis (i.e. the sagittal or xz-plane) of the radial coordinate system (3). (In this system, 90° represents a motion of pure radial/ulnar deviation, 45° describes a motion involving equal parts flexion extension to radial/ulnar deviation, and 0° represents pure flexion/extension.)

Wrist motion can not be fully defined by direction alone, just as a line can not be completely defined by its slope. A line is typically described by *both* its slope and its y-intercept. When describing a path of wrist motion, the “y-intercept” is the flexion/extension offset. This flexion/extension offset is defined as the wrist position in flexion/extension when the wrist is in neutral radial/ulnar deviation. Without including this flexion/extension offset, direction of wrist motion would describe an infinite number of parallel paths.

2.3.5 Statistical Analysis

Wrist range of motion was reported as the mean \pm SD of the difference between the two most extreme wrist positions (full windup and full impact). Forearm range of motion was also reported as a mean \pm SD of the difference in forearm pronation/supination posture between the two most extreme wrist positions.

A single hierarchical linear model (HLM) (14) was used to calculate the overall coupling ratio for the hammering task as well as the flexion/extension offset during hammering. The HLM provided estimates of the between-subject variability (standard

error), as well as the significance of the coupling ratio, using threshold of $p < 0.05$ established *a priori*. A second HLM was used to test for a relationship between forearm pronation/supination and wrist flexion/extension ($p < 0.05$).

The percent contribution of the scaphoid and lunate to overall wrist motion (radio-scaphoid and radio-lunate rotation) were each calculated using an additional HLM. The threshold for a significant relationship was established at $p < 0.05$ *a priori*. To understand how the direction of wrist motion, or the wrist coupling ratio, affects the amount of radiocarpal rotation we used a piecewise mixed effects model (15). In this model, the direction of wrist motion for each subject was compared to that subject's percentage of radio-scaphoid and radio-lunate rotation.

2.4 Results

2.4.1 Wrist and Forearm Motion

Average range of motion from full windup to full impact was $70 \pm 10^\circ$. The flexion/extension to radial/ulnar deviation coupling ratio for wrist motion during hammering was 1.2 ($p < 0.01$) with a standard error of 0.12. Practically, this means that for every 10° of wrist ulnar deviation there was approximately 12° of wrist flexion (**Figure 2.2**). This corresponds to a path of wrist motion oriented 41° from the sagittal plane. The flexion/extension offset was determined to be 54° of wrist extension, meaning when the wrist was in neutral radial/ulnar deviation, it is 54° extended.

There was minimal forearm pronation/supination during hammering, averaging only $12 \pm 8^\circ$ of overall rotation from full windup to full impact. There was no significant coupling ratio between pronation/supination and flexion/extension ($p = 0.12$) (**Figure 2.3**). While the amount of pronation/supination was minimal during our simulated hammering task, the forearm position of our volunteers during this task was quite variable, ranging from 60° of pronation to 36° of supination (average $1 \pm 32^\circ$ pronation) in the neutral position.

2.4.2 Radiocarpal Motion

During hammering, the rotation of the scaphoid with respect to the radius was non-zero ($p < 0.01$), and contributed approximately 40% (standard error 5%) of the wrist motion (i.e. for every 10° of wrist rotation, the scaphoid rotated on average 4°).

Similarly, lunate rotation was also non-zero ($p < 0.01$), contributing 41% (standard error 4%) of the overall wrist rotation. These percentages indicate that approximately 60% of the total wrist motion occurred at the midcarpus (**Figure 2.4**). Scaphoid and lunate translations were 0.5 ± 0.4 mm and 0.6 ± 0.5 mm, respectively, throughout the entire task, confirming, as expected, that the majority of radiocarpal motion was rotation.

Our mixed effect modeling suggested that the path of wrist motion during hammering influenced the magnitude of radioscaphoid rotation. When radioscaphoid rotation was plotted as a function of wrist motion, there was a clear bimodal trend. Each half of this trend was represented as a linear regression connected at an inflexion point (**Figure 2.5a**). The inflexion point for radio-scaphoid rotation was located at the path of wrist motion oriented 32° from the sagittal plane, which corresponds to a coupling ratio of 1.6. As the hammering path deviated from that path towards one with relatively more radial/ulnar deviation, the amount of radioscaphoid rotation increased. As the path deviated towards one with relatively more flexion/extension, the results tended towards increased radioscaphoid rotation. When analyzing lunate motion, the mixed effect model failed to converge, which indicated that there was no inflection point within the data set (**Figure 2.6a**). In this case, linear regression revealed that radiolunate rotation decreased monotonically as the path of wrist motion moved towards flexion/extension.

2.5 Discussion

This study was performed to investigate the path of wrist and forearm motion and radioscaphoid and radiolunate rotation during *in vivo* hammering. We found that the path of wrist motion during a simulated hammering task followed a path oriented 41° from the sagittal plane and took place with the wrist held almost entirely in extension. Radiocarpal motion was reduced to 40% of overall wrist motion.

The average hammering path during our study was similar to the paths of hammering previously reported (1, 4), as well as the DTM reported in previous studies (5, 8). These studies have all reported paths of wrist motion that range between 37° and 50° from the sagittal plane.

Traditionally, the DTM has been reported in terms of the direction of wrist motion or the ratio of flexion to ulnar deviation during motion. Most studies have focused solely on the direction of wrist motion and have not analyzed or reported any flexion/extension offset during the motion. However, there is increasing evidence that hammering takes place along a dart-thrower's oriented path that does not pass through a neutral wrist position, rather through a largely extended wrist position (1, 4). This path is parallel to the paths of dart throwing motions previously studied (involving the same or similar directions of wrist motion). However, it is clearly a different wrist motion, and likely involves different carpal kinematics.

Previous studies have shown dart throwing motions which used minimal scaphoid and lunate rotation (5, 8). In this study, radiocarpal motion was on average 40% of overall wrist motion. This larger than expected radioscaphoid rotation may have been

caused by a variety of factors. The large flexion/extension offset (54° extension) could have caused our results to differ from prior studies. It is also possible that the hammering paths used by our subjects deviated from the DTM which minimizes radioscaphoid rotation. There are also clear limitations with comparing our static simulation to dynamic hammering.

We acknowledge that our measurement of carpal kinematics during simulated hammering using a CT-based method is limited in that it infers dynamic data from static CT positions. However, we choose this method because it is currently the most accurate non-invasive method capable of measuring the complex 3-D motions of the carpal bones *in vivo*. There is also a chance that the use of an unweighted hammer handle might affect our calculated motion. However, we justified the use of our method in a pilot kinematic study that showed the wrist follows a similar path during a simulated hammering motion as during dynamic hammering (Curran PF, Rainbow MJ, Moore DC, Crisco JJ. Hammering and Dart Throwing are Kinematically Different. American Society of Biomechanics; 2007). This was done using MTx Inertial Measurement Units (Xsens Technologies B.V., The Netherlands), and gave us confidence that our CT data would be representative of dynamic hammering.

One of our most interesting findings was that the specific path of wrist motion has an effect on radioscaphoid rotation during hammering. Our piecewise modeling (**Figure 2.5a**) showed that radioscaphoid rotation decreased as wrist motion changed from pure ulnar deviation to one that involves radial extension to ulnar flexion. Further, we found that there is a clear inflexion point when the path of wrist motion reaches 32° from the sagittal plane. Beyond 32° , towards a more flexion-dominated motion, the results were

less clear. However, the regression did trend towards increased radioscapoid rotation as wrist motion moved towards pure extension. The lack of clarity was due to the fact that only four of our volunteers hammered along paths beyond 32° , and the paths of these four subjects were all closely clustered within 5° of each other, making the regression less compelling.

Our data is very consistent with the findings of Werner et al. (5). They measured radioscapoid and radiolunate rotation during 9 paths of wrist motion using 5 cadaver wrists. They found that minimal scaphoid rotation was 26% of overall wrist motion, and took place during a path of wrist motion 45° from the sagittal plane. However, when we analyze their data using our piecewise model, we found a similar pattern between the regression lines (**Figure 2.5b**). Both sets of data show that radioscapoid rotation is minimized along a path of motion involving a combination of flexion and ulnar deviation and increases as the path of motion deviates from that inflexion point. This trend is represented by the “V” shaped regressions in both graphs. Performing the same analysis on Werner et al.’s radiolunate rotation data radiolunate rotation helps to explain our findings regarding radiolunate rotation (**Figure 2.6a**). In Werner et al.’s data (**Figure 2.6b**) the unmistakable “V” shape is apparent; however, the inflexion point has shifted towards a pure flexion motion by 12° compared to the scaphoid inflexion point. When that same shift is applied to the inflexion point of our scaphoid data (32°), we predict that the inflexion point for radiolunate rotation should occur at a 20° path of wrist motion. When we consider that this path is 6° beyond the most extreme path of any of our subjects, it becomes clear why the piecewise mixed effect model failed to converge. All of our subject’s hammering paths were oriented more towards radial/ulnar deviation than

the predicted inflexion point, or the predicted path which minimizes lunate rotation. As such, all of the data points in Figure 2.6a represent only the left half of the expected trend or the left half of the “V”. The left half of the “V” is a simple line, which was modeled correctly using linear regression. Our results provide additional support for the observations that the path of wrist motion that minimizes radioscapoid rotation differs by approximately 10° from that which minimizes radiolunate rotation (3, 5, 8).

The piecewise modeling results suggest that most of our subjects “hammered” along paths biased slightly more towards ulnar deviation than paths that completely minimize radioscapoid rotation (and still further from the path that minimizes radiolunate rotation). It is interesting that most subjects used paths that failed to minimize rotation of either the radius or the scaphoid. Minimizing rotation of these two bones at the radiocarpal joint has been theorized to have given humans an evolutionary advantage by creating a more stable wrist joint for high demand activities such as clubbing and hammering (16). It may be that because our volunteers were novices at hammering, they did not choose optimal hammering paths and that more experienced hammerers would follow paths that would, in fact, minimized radiocarpal rotation. That’s possible. However, there may not be one single hammering motion. In fact, there is good data to suggest that there are distinct differences in the direction of wrist motion for overhead hammering versus bench-top hammering (1). While both types of hammering appear to involve radial extension to ulnar flexion (generally the DTM), it is clear that both motions cannot minimize radiocarpal motion.

While it has been hypothesized that hammering involves supination of the wrist and forearm (3), our results do not support this hypothesis. While the forearm orientation

varied among the subjects, we found that pronation/supination motion was minimal during our simulated hammering task. It is possible that this finding is a result of our experimental setup. By carefully controlling the experimental setup, and aligning the shoulder, elbow, and wrist with the hammering swing, we could have caused a reduction in the amount of forearm rotation normally associated with dynamic hammering. To the best of our knowledge, however, no one has yet reported pronation/supination data during hammering or any other functional task, so we have no real reference standard by which to compare our data.

In vivo measurement of carpal motion during functional tasks is critical to our understanding of carpal function, and for the development of rehabilitation protocols customized to specific injuries, surgery and occupation.

2.6 References

1. Schoenmarklin, R.W. and Marras, W.S., *Effects of handle angle and work orientation on hammering: I. Wrist motion and hammering performance*. Hum Factors, 1989. **31**(4): 397-411.
2. Capener, N., *The hand in surgery*. J Bone Joint Surg Br, 1956. **38-B**(1): 128-151.
3. Moritomo, H., Apergis, E.P., Herzberg, G., Werner, F.W., Wolfe, S.W., and Garcia-Elias, M., *2007 IFSSH committee report of wrist biomechanics committee: biomechanics of the so-called dart-throwing motion of the wrist*. J Hand Surg [Am], 2007. **32**(9): 1447-1453.
4. Palmer, A.K., Werner, F.W., Murphy, D., and Glisson, R., *Functional wrist motion: a biomechanical study*. J Hand Surg [Am], 1985. **10**(1): 39-46.
5. Werner, F.W., Green, J.K., Short, W.H., and Masaoka, S., *Scaphoid and lunate motion during a wrist dart throw motion*. J Hand Surg [Am], 2004. **29**(3): 418-422.
6. Moritomo, H., Murase, T., Goto, A., Oka, K., Sugamoto, K., and Yoshikawa, H., *In vivo three-dimensional kinematics of the midcarpal joint of the wrist*. J Bone Joint Surg Am, 2006. **88**(3): 611-621.
7. Ishikawa, J., Cooney, W.P., 3rd, Niebur, G., An, K.N., Minami, A., and Kaneda, K., *The effects of wrist distraction on carpal kinematics*. J Hand Surg [Am], 1999. **24**(1): 113-120.
8. Crisco, J.J., Coburn, J.C., Moore, D.C., Akelman, E., Weiss, A.P., and Wolfe, S.W., *In vivo radiocarpal kinematics and the dart thrower's motion*. J Bone Joint Surg Am, 2005. **87**(12): 2729-2740.
9. Goto, A., Moritomo, H., Murase, T., Oka, K., Sugamoto, K., Arimura, T., Masumoto, J., Tamura, S., Yoshikawa, H., and Ochi, T., *In vivo three-dimensional wrist motion analysis using magnetic resonance imaging and volume-based registration*. J Orthop Res, 2005. **23**(4): 750-756.
10. Crisco, J.J., McGovern, R.D., and Wolfe, S.W., *Noninvasive technique for measuring in vivo three-dimensional carpal bone kinematics*. J Orthop Res, 1999. **17**(1): 96-100.
11. Gonzalez-Ochoa, C., McCammon, S., and Peters, J., *Computing Moments of Objects Enclosed by Piecewise Polynomial Surfaces*. ACM Transactions on Graphics (TOG), 1998. **17**(3): 143-157.
12. Coburn, J.C., Upal, M.A., and Crisco, J.J., *Coordinate systems for the carpal bones of the wrist*. J Biomech, 2007. **40**(1): 203-209.
13. Li, Z.M., Kuxhaus, L., Fisk, J.A., and Christophel, T.H., *Coupling between wrist flexion-extension and radial-ulnar deviation*. Clin Biomech (Bristol, Avon), 2005. **20**(2): 177-183.
14. Bryke, A.S. and Raudenbush, S.W., *Hierarchical Linear Models: Applications and Data Analysis Methods*. 1992, Thousand Oaks, CA: Sage Publications. 265.
15. Naumova, E.N., Must, A., and Laird, N.M., *Tutorial in Biostatistics: Evaluating the impact of 'critical periods' in longitudinal studies of growth using piecewise mixed effects models*. Int J Epidemiol, 2001. **30**(6): 1332-1341.

16. Wolfe, S.W., Crisco, J.J., Orr, C.M., and Marzke, M.W., *The dart-throwing motion of the wrist: is it unique to humans?* J Hand Surg [Am], 2006. **31**(9): 1429-1437.

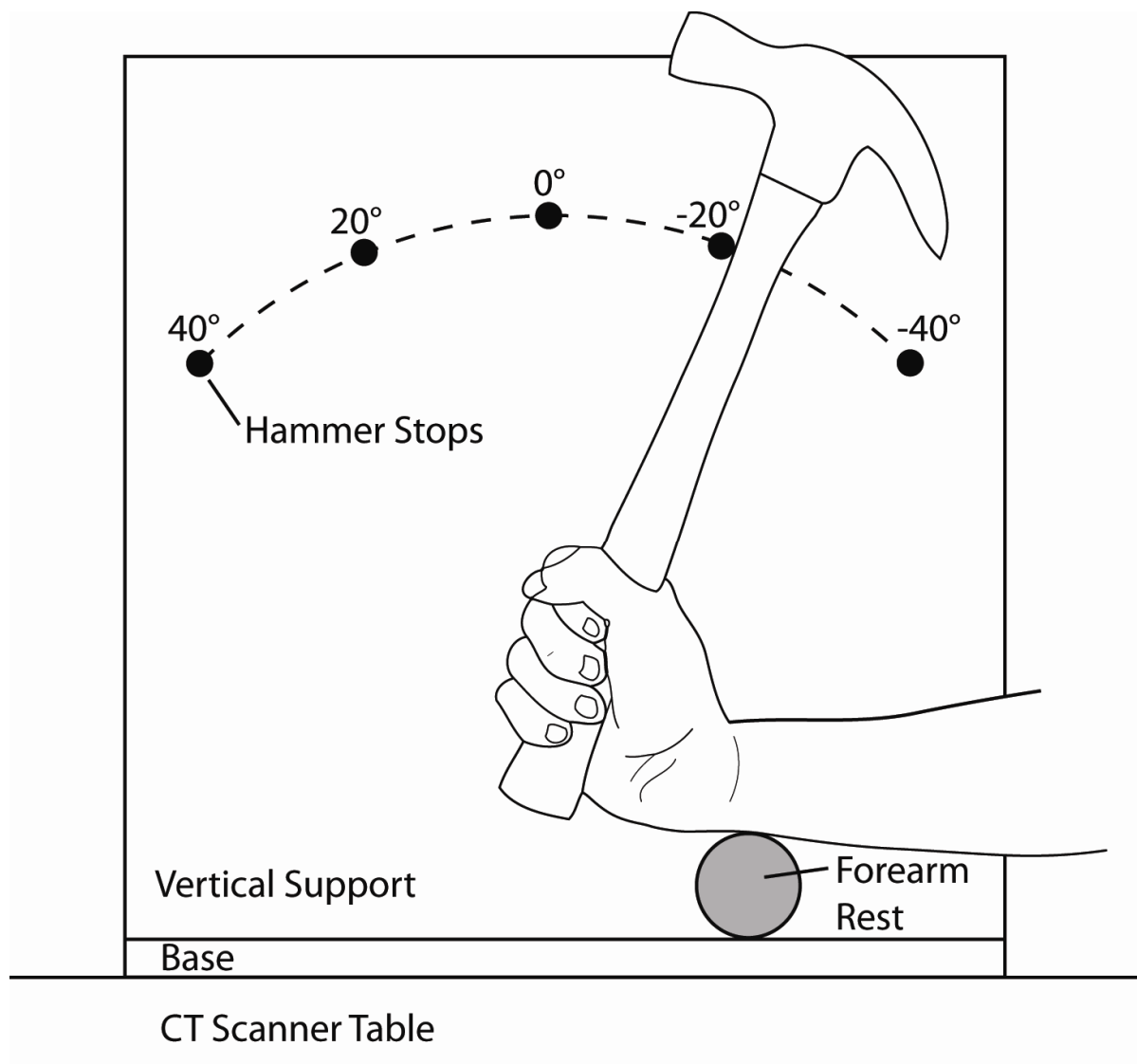


Figure 2.1. Drawing of the hammering jig used during CT scanning. The dominant hand of each subject was supported by a forearm rest. To minimize motion during scanning, the jig was equipped with stops for the hammer handle at each of the 5 hammering positions. Each stop was a 4" long, ½" diameter dowel. The head of the hammer was removed prior to scanning, and was included in the figure for illustration purposes.

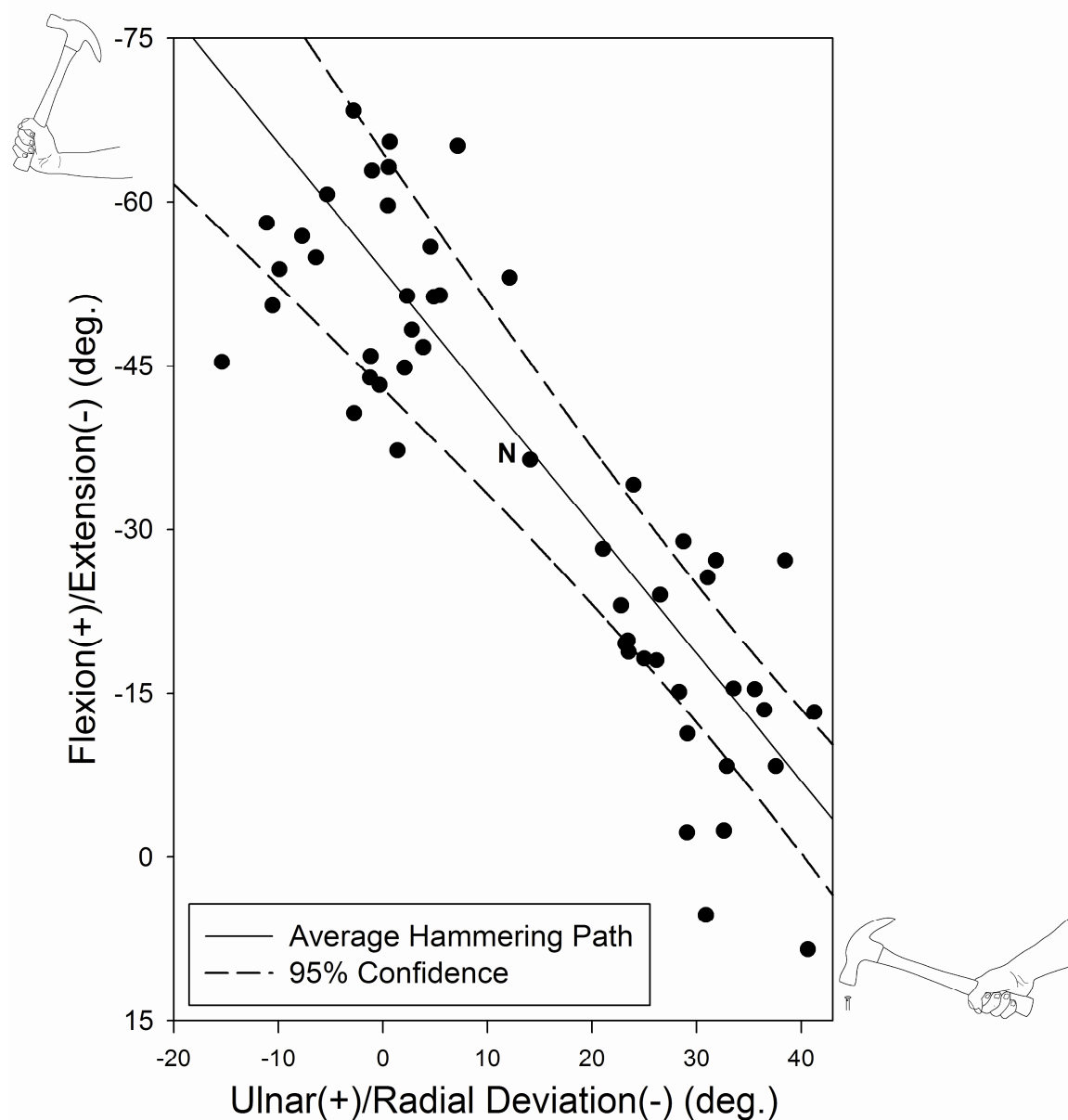


Figure 2.2. Wrist positions during hammering followed a path from radial-extension to ulnar-flexion, a motion also referred to as the Dart Thrower's path. These positions were normalized such that the neutral hammering position of each subject was located at the (N) average neutral hammering position for visualization purposes only.

Pronation & Supination Durring Hammering

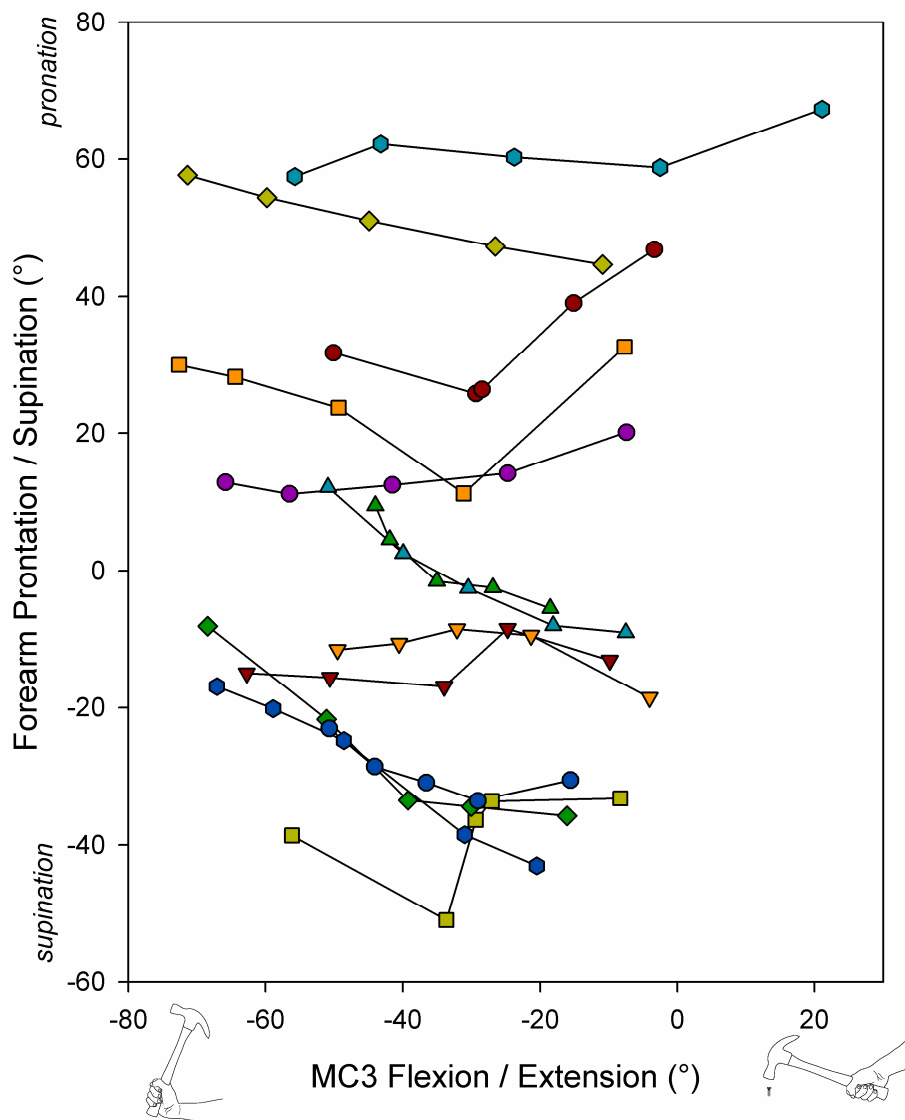


Figure 2.3. There was minimal pronation/supination during hammering. Each subject rotated on average only 12° throughout the entire rand of motion.

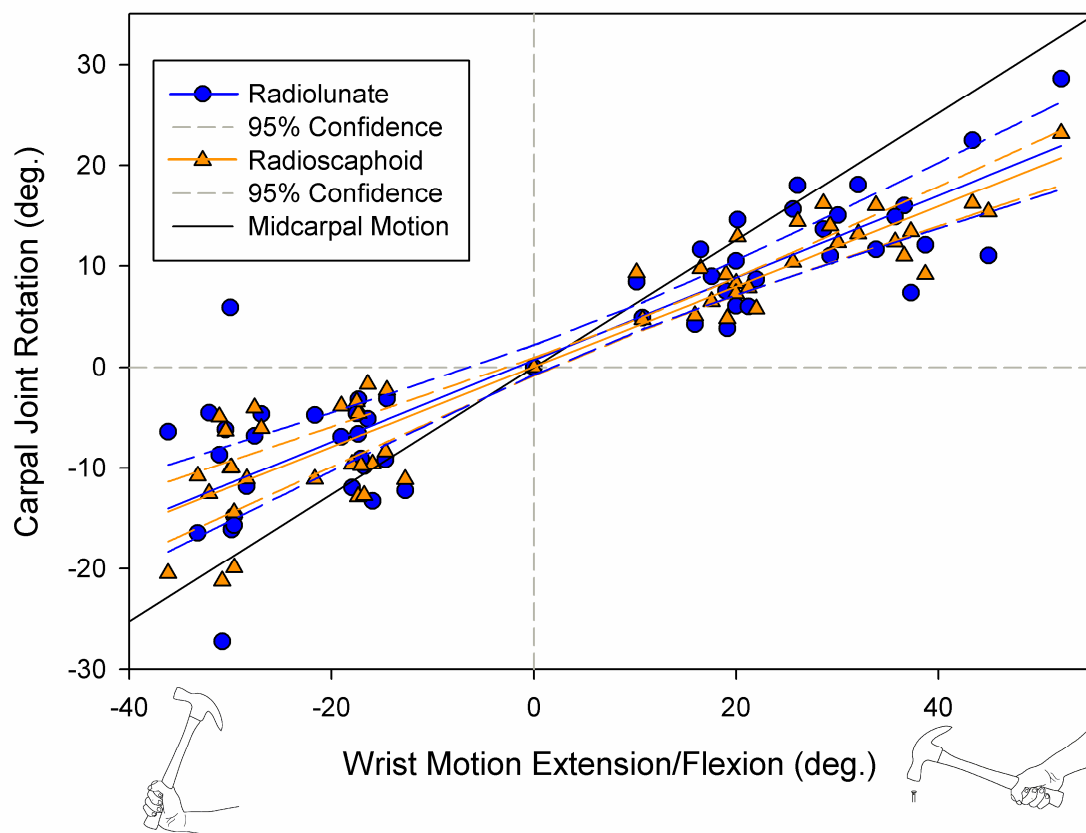


Figure 2.4. During hammering scaphoid and the lunate rotation was 40% and 41% of wrist motion respectively.

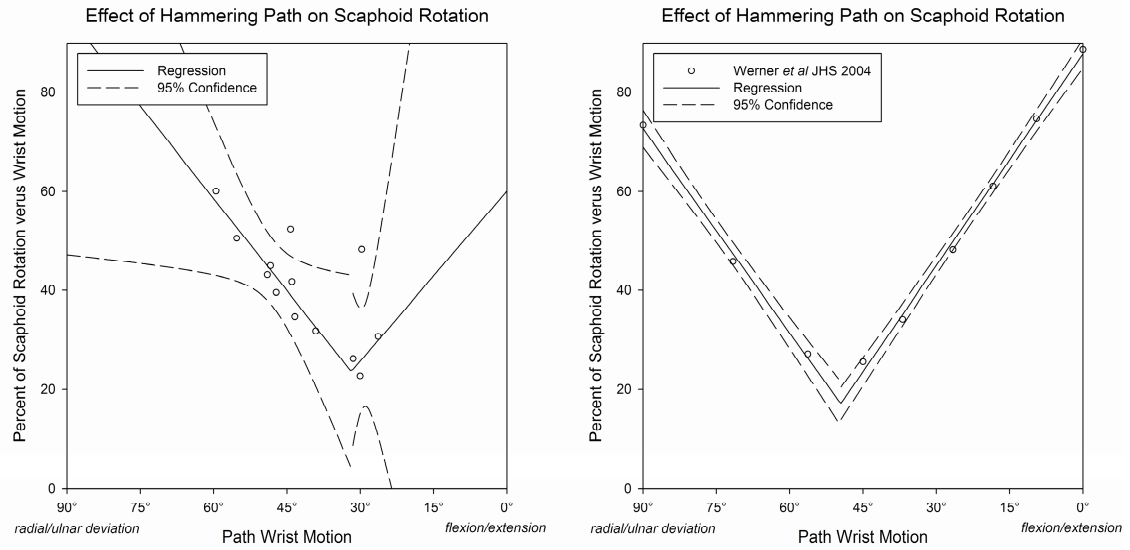


Figure 2.5. a) Each subject's path of wrist motion, or the coupling ratio, affected that subject's amount of residual radioscaphoid rotation during hammering. Radioscaphoid rotation was minimized at a path of 32° from the sagittal plane; as subjects moved away from that DTM, radioscaphoid rotation increased. b) These results were similar to those of Werner et al. (adapted from Werner et al.)

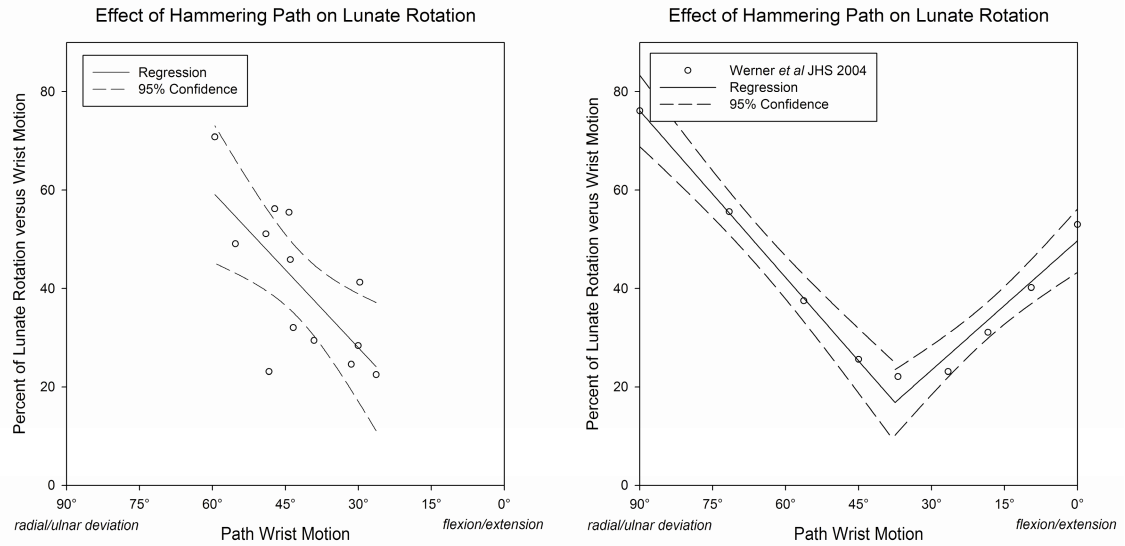


Figure 2.6. a) Increasing amount of flexion/extension in paths of global wrist lead to a decrease in the amount of radiolunate rotation. b) When compared to the results of Werner *et al.*, it suggests that the hammering paths of our subjects were too far towards radial/ulnar deviation to detect the path which minimizes radiolunate rotation. (adapted from Werner *et al.*)

Chapter 3

Conformational Carpal in the Carpus During Finger Traps

Evan L. Leventhal, Douglas C. Moore, Edward Akelman, Scott W. Wolfe
and Joseph J. Crisco

The following chapter is in preparation for submission to the *Journal of Hand Surgery*.

3.1 Abstract

3.1.1 Introduction

Wrist distraction is a provocative maneuver used clinically for the treatment of distal radial fractures, during arthroscopy and as a test for scapholunate ligament injury. The purpose of this study was to measure the 3-D changes in the healthy carpus as a results of a static distractive load.

3.1.2 Methods

The dominant wrists of 14 healthy volunteers were scanned using computed tomography during a distractive task at both 0N and 98N of load. Load was applied using finger traps and volunteers were encouraged to relax their forearm muscles and allow subluxation of the wrist. The motions of the bones in the wrist were tracked between the unloaded and loaded trial using markerless bone registration. The average displacement vector of each bone was calculated relative to the radius as well as the interbone distances for 20 bone-bone interactions. Joint separation was estimated at the radiocarpal, midcarpal and carpal-metacarpal joints in the direction of loading using the radius, lunate, capitate and 3rd metacarpal.

3.1.3 Results

After loading the distance between the radius and 3rd metacarpal increased an average of 3.3 ± 3.1 mm in the direction of loading. This separation was primarily located at the radiocarpal (1.0 ± 1.0 mm) and midcarpal (2.0 ± 1.7 mm) joints. There was minimal lateral changes within the distal row, although the proximal row narrowed by 0.98 ± 0.7 mm. Distraction of the scaphoid (2.5 ± 2.2 mm) was 2.4 times greater than the lunate (1.0 ± 1.0 mm).

3.1.4 Conclusions

Carpal distraction has a significant effect on the conformation of the carpus, especially at the radiocarpal and midcarpal joints. Surgeons should be aware that external traction causes twice as much distraction at the lunocapitate joint than at the radiolunate joint.

3.2 Introduction

The wrist is a uniquely passive joint; the motion of individual carpal bones is almost entirely driven by their shape and the extrinsic and intrinsic ligaments of the wrist. The pattern of conformational changes within the carpus during distraction is therefore largely dependent upon the ligaments.

Despite their importance, little is known about the mechanical properties of the carpal ligaments. Most of our understanding of carpal ligaments is derived from careful dissection (1, 2), limited mechanical testing (3-5), and measuring alterations in kinematics after sectioning ligaments in cadaveric models (6-8). A potentially more powerful technique to analyze ligament function is use of computer modeling combining 3-D bone kinematics and ligament insertions sites (9, 10). To date, the kinematic data driving these models has been largely derived from range of motion studies, primarily in the flexion/extension and radial/ulnar deviation planes of motion.

Axial wrist distraction is a provocative intervention that may provide foundational data for additional ligament analysis. Existing biomechanical studies of carpal distraction have been almost entirely limited to two-dimensional analysis using plain radiographs (11-13). Most studies have focused on radiocarpal joint spacing and did not measure any rotational changes. The three dimensional effects of distractive loads on the carpus have only been measured in a single cadaveric study (14), where the authors demonstrated that distraction reduces radiocarpal motion during extension and increases radiocarpal motion during flexion.

Mechanical testing of cadaveric wrists under distraction showed a wide variability in the amount of distraction between wrists (11), but did not attempt to correlate those differences with gender. Ligament laxities in the knee and other joints have been shown to be greater in women than men (15-17), but this difference has not been confirmed in the wrist. Assuming that ligaments are the limiting factor in carpal distraction, it is possible that women exhibit greater excursion during distraction.

External traction of the wrist has been shown to assist in the reduction of intra-articular fractures. Ligamentotaxis is used to transmit the external force across the carpus and assist alignment of distal radial fractures (18). While distraction has been shown to assist in fracture reduction, the load and duration of use has also been negatively associated with outcome measures such as wrist and finger motion, pain, function and grip strength (19).

Distraction is also used clinically during arthroscopy as well as in the diagnosis of injury to the scapholunate ligament injury (12, 13). While two groups have claimed success in diagnosing ligament injury using distraction, an earlier study showed variable sensitivity and specificity with a similar technique and concluded that such testing was not useful for the diagnosis of chronic wrist pain (20).

Accurate data on carpal changes due to distraction has applications for clinicians and basic scientists. Possible that this data could help explain the negative outcomes associated with distraction. Improved understanding of how the healthy wrist behaves under distraction allows for more accurate interpretation of distractive tests used in the diagnosis of ligament injury. Finally, recording the 3-D bone kinematics of the wrist

before and after loading can be used with existing computer models to improve our understanding of the mechanical properties of the carpal ligaments.

We were interested in the three-dimensional effects of distraction on the *in vivo* carpus when the forearm muscles were relaxed and the wrist is allowed to sublux. Knowing that the size of the carpal bones vary with gender (21), we were also interested in determining if there was any correlation between gender and the amount of distraction. The purpose of our study was to measure the 3-D changes in the healthy carpus as a results of a static distractive load.

3.3 Methods

3.3.1 Volunteer Recruitment and CT Scanning

After obtaining IRB approval, 14 healthy right-hand dominant volunteers (7 male and 7 female; average age 24.9 years, range 21-30) were recruited. Volunteers were prescreened for history of wrist injury or wrist surgery. Volunteers were also excluded for metabolic disease which could alter soft tissue structures in the wrist.

Nylon finger traps were used to apply a distractive load across all 5 fingers. Volunteers were positioned prone on the scanning table, with their right arm extended above their head and oriented down the length of the table. To minimize wrist motion between the unloaded and loaded scans, the distraction load was briefly applied prior to scanning the wrist in the unloaded trial. The load was then removed immediately prior to scanning. During the loaded trial, volunteers were instructed to relax their forearm muscles and allow the load to sublux their wrists.

Computed tomography images were generated for each subject in both an unloaded and loaded state. In the loaded trial, a 98N (10kg) distraction force was applied parallel to long axis of the arm. The 98N load represented the maximum load that could be comfortably held by volunteers and is a load used in previous studies (22-25). A third CT scan was collected of the neutral wrist for segmentation. Scanning was performed using a GE LightSpeed 16, at 80kVp and 80mA. In plane resolution was 0.3mm x 0.3mm with a slice interval of 0.6mm.

3.3.2 Carpal Tracking

Carpal kinematics between loaded and unloaded wrist positions were calculated using our established markerless bone registration methodology. In brief, the radius, ulnar, carpal bones, and metacarpals for each volunteer were manually segmented from the neutral position to create 3-D bone cortical surface models using Mimics 9.11 (Materialise, Leuven, Belgium). Bone centroids and inertial axes were calculated based the 3-D surface models of each bone from the neutral wrist(26, 27). The location of each bone in the unloaded and loaded position was then identified using custom C++ software (GNU gcc, Free Software Foundation, Boston, Massachusetts). The radii in the unloaded and loaded positions were then registered to the radius in the neutral scan to eliminate any forearm motion between scans using custom Matlab code (The MathWorks, Natick, Massachusetts).

To create a common reference frame for comparison between subjects, a radius-based coordinate system (RCS) was defined for each subject using an existing methodology (28, 29). This coordinate system was created for each volunteer using anatomic landmarks of the radius. The x-axis was oriented proximally, aligned with the long axis of the distal radial diaphysis. The y-axis was oriented in the radial direction, calculated as a vector orthogonal to the x-axis and passing through the radial styloid. Finally the z-axis was oriented volarly, calculated as the vector orthogonal to both the x and y-axis. The origin of the coordinate system was located at the point on the cortical surface of the radius intersected by the x-axis. The origin is located on the ulnar edge of the radioscaphoid fossa. A similar coordinate system was defined for the ulna, with the y-axis oriented towards the ulnar styloid instead of the radial styloid.

Wrist position was defined by the orientation of the 3rd metacarpal's long inertial axis with respect to the radial coordinate system. Forearm pronation/supination was measured as the rotation of the radius about the ulna. Individual bone rotations were calculated using helical axis of motion variables. Rotations were represented as their unsigned magnitude as well as broken down into components of rotation in flexion/extension, radial/ulnar deviation and pronation/supination.

3.3.3 Outcome Variables

3.3.3.1 Bone Centroid Displacement

The displacement of each bone centroid due to loading was computed as the difference in centroid position vectors between unloaded and loaded positions. The magnitude of displacement vector represented the distance the centroid moved. Direction of displacement vector was described in the radial coordinate system as its orientation in flexion/extension and radial/ulnar deviation. Centroid calculation or point selections were only calculated once for each subject in the unloaded position. Centroid location in the loaded position was calculated using the 3-D kinematics derived from motion tracking.

Since centroids could not be accurately computed for the partially scanned long bones, alternate points were used instead. For the radius and ulna, the origins of their respective coordinate systems were used to defined their “centroid”. For the metacarpals, points were manually selected on the metacarpal head in the center of its articular surface to represent its “centroid”. Point selection was only performed once per bone. The location of each point in the loaded position was calculated using the 3-D kinematic data.

3.3.3.2 Centroid Distances

Centroid distance was defined as the change in length between the centroids of two bones, and was described for 20 bone-bone combinations (**Table 3.1**). Change in centroid distance was reported as the difference between the loaded centroid distance and the unloaded centroid distance, with positive values indicating a separation of the two bones

The 20 bone-bone interactions were selected to give an overview of the changes taking place within the wrist due to loading. In addition to the 20 bone-bone interactions, lateral changes were approximated for the proximal and distal rows. Overall change in lateral distance for the proximal row was computed as the centroid distance between the scaphoid and triquetrum. Similarly, lateral distance at the distal row was computed as the centroid distance between the trapezium and hamate.

3.3.3.3 Joint Separation

For a more clinically relevant outcome measure, we approximated the joint separation that can be measured on a posteroanterior radiograph for four joints. This measurement was similar to centroid distance; however, changes were only measured in the direction of loading, or along the distal-proximal coordinate axis (x-axis) or the radius-based coordinate system.

Joint separation was measured at the radiolunate, radioscapoid, lunocapitate, and 3rd carpal-metacarpal joints. Radiocarpal joint distance was defined as the distance between the centroids of the radius and the lunate. Midcarpal distance was defined as the

distance between the centroids of the lunate and capitate. Finally, carpal-metacarpal distance was defined as the distance between the centroids of the capitate and 3rd metacarpal. Total wrist distraction was measured as the change in distance between the centroids of the radius and 3rd metacarpal.

3.3.4 Statistics

To determine if there were significant changes in the wrist position after loading, the flexion/extension component of wrist position in the unloaded posture was compared to the position in the loaded posture using a paired Student's t-test. Similar comparisons were made for the radial/ulnar component of wrist position as well as the forearm pronation/supination position before and after loading.

Joint separation at the radiolunate, radioscapoid, lunocapitate, and 3rd carpal-metacarpal joints were evaluated using 3-factor mixed linear model, with one between-subject factor (gender) and two within-subject factors (joint and loading). We used SAS *proc mixed* (SAS, Cary, NC) with an unstructured variance-covariance error structure for bone x loading within subject.

3.4 Results

3.4.1 Wrist Position and Carpal Rotation

The position of the average unloaded wrist was $2\pm 8^\circ$ flexed and $8\pm 6^\circ$ ulnarly deviated. After loading wrist position changed an average of $6\pm 5^\circ$ from the unloaded wrist posture. The loaded wrist was ulnarly deviated $3\pm 3^\circ$ from the unloaded position ($p<0.01$). After loading, the forearm rotated $5\pm 6^\circ$ in pronation/supination, but there was no significant change in the forearm position after loading ($p=0.09$). There was no significant change in the flexion/extension position of the wrist ($p=0.09$).

Average rotation of individual carpal bones was less than 10° after loading. When broken down into components of rotation, no bone averaged more than 4° of rotation in any given direction and the average across all bones and subjects less than 2° of rotation in flexion/extension and pronation/supination and less than 1° of rotation in radial/ulnar deviation.

3.4.2 Bone Translation

Centroid displacement was generally in the direction of load and slightly dorsal. Average bone displacement ranged from only the 2mm translation for the lunate, to more than 6mm translation for the 1st metacarpal. Interestingly, both the lunate and triquetrum had larger components of radial translation than any of the other bones (**Figures 3.1 & 3.2**) (**Table 3.2**).

3.4.3 Centroid Distances

Centroid distances generally increased throughout the wrist. The only major decrease in distance was between the centroid of the radius and lunate. The changes in centroid distances within the distal row were all less than 0.25mm. There was even less change within the proximal row, with all changes less than 0.1mm (**Figure 3.3**) (**Table 3.1**).

The overall lateral distance across the proximal row decreased 0.98 ± 0.7 mm after loading. There was less change in the overall lateral distance of the proximal row, increasing 0.17 ± 0.3 mm.

3.4.4 Joint Separation

After tensile loading, overall interbone distance across the carpus (radius-3rd metacarpal) increased by an average of 3.3 ± 3.1 mm. Separation was clearly visible at the radiolunate and lunocapitate joints (**Figure 3.3**). There was no significant relationship between gender and distraction ($p=0.26$). At the radiolunate joint, distraction significantly ($p<0.01$) increased interbone distance by 1.0 ± 1.0 mm. At the radioscapoid joint, distraction significantly ($p<0.01$) increased interbone distance by 2.5 ± 2.2 mm. The interbone distance between the lunate and the capitate also increased significantly ($p<0.01$) after distraction, by 2.0 ± 1.7 mm. Interbone distance at the 3rd carpal-metacarpal joint increased by 0.2 ± 0.5 mm, but was not significant ($p=0.07$).

The change in interbone distance at the lunocapitate joint was significantly greater ($p<0.01$) than at the radiolunate joint. The change in interbone distance at the 3rd carpal-metacarpal joint with distraction was significantly less than at the change at the radiolunate ($p<0.01$) and lunocapitate ($p<0.01$) joints (**Figure 3.4**).

3.5 Discussion

This study was designed to determine how static distraction affects the carpus. Under 98N of distractive load, we found the entire carpus separated 3.3mm primarily over the radiocarpal and midcarpal joints. There was relatively little separation at the carpal-metacarpal joint. Almost all of the bones in the carpus exhibited some degree of dorsal motion, with the more distal bones generally moving more. At the proximal row, the scaphoid distracted the most while both the lunate and the triquetrum moved radially as they distracted. This lateral motion resulted in a narrowing of the proximal row.

The radiolunate joint was the only bone-bone interaction to have a major decrease in centroid distance. In this case, the distance between the surfaces of these two bones actually increased. However, the lunate centroid started quite ulnar of the radius centroid and moving radially during distraction. This radial motion of the lunate caused an apparent decrease in distance between the bone centroids which overshadowed the separation of the lunate from the radius.

Rotation of individual bones in the carpus was relatively small. While the total amount of rotation for any given bone was almost 10° , there was no consistent pattern of rotation. This is highlighted by the fact that the average bone rotation in any given direction was less than 2° .

The ability to interpret the relative distraction of different carpal bones is improved by an understanding of the ligament anatomy. That distraction was greatest at the radiocarpal and midcarpal joints is not necessarily unexpected, given the significant mobility of the scaphoid, lunate and capitate during normal wrist motion (30, 31).

Several authors have suggested that this mobility at the radiocarpal and midcarpal joints can be explained by the ligamentous structure on the volar and dorsal aspects of the wrist. The four primary volar ligaments are arranged to form two inverted V's. The smaller V is formed by the radiolunate and ulnolunate ligaments, both of which insert on the lunate, and branch out towards the radius and ulnar respectively. The larger V, comprised of the radioscapohamate and arcuate ligaments, follows a similar path, but starts further laterally on the radius and ulna and inserts onto the capitate (2, 32-34). It is important to recognize that all of these ligaments are oriented at a significant angle relative to the direction of load, thus allowing a certain degree of distraction with only minimal elongation. On the other hand, limited distraction at the carpal-metacarpal joint is explained by the tight ligamentous attachments and coupling of the capitate to third metacarpal during normal wrist motion (35).

It remains unclear why most of the carpal bones translated dorsally after distraction. Various authors have described the volar ligaments as being stronger than the dorsal ligaments, which form a 'Z' shape on the dorsal side of the wrist (32). These authors suggested that distraction is arrested by the volar ligaments before the dorsal ligaments reached their maximum length (14, 36, 37). Assuming that it is the volar ligaments that are restraining distraction, then those bones would be expected to translate volarly, in the direction towards their attachments if they were going to move at all.

Our measured distraction is similar to those previously reported. Bartosh and Saldana (37) found an average of 3mm of distraction in 19 cadaver wrists, regardless of the amount of load used. Loebig et al. (11), performed distraction on 12 cadaveric wrists using a mechanical testing device. While, they measured more than twice as much

distraction (almost 8mm) at 98N of load than in our study, they removed all skin and soft tissue (including muscles and tendons) except for the wrist capsular ligaments. Direct comparisons of interbone distances are not possible because of differences in methodologies. Instead, it is possible to compare the relative motion of bones at a given distraction distance. At 3.3mm of distraction (the average for our subjects), Loebig et al. found that lunocapitate distraction was 2.4 times as much as radiolunate distraction. This is only slightly different from our finding of 2.0 times the distraction. Comparing the ratio of distraction at the radioscapoid joint to radiolunate joint, they reported roughly 2.2 times greater motion at the radioscapoid joint, while our study measured 2.4 times greater motion.

There was no difference in the amount of distraction between males and female volunteers. While prior studies have documented differences in the size of the carpal bones with gender (21), it is unclear if that would translate to differences in distractive loads. It is possible that there are very small differences that would only be seen with a significantly larger study.

Ligamentotaxis during carpal distraction causes more separation at the midcarpal joint than at the radiocarpal joint. Clinically, carpal distraction is used in the treatment of comminuted distal radial fractures (18). Previous studies have shown that distraction of the wrist to be a potential source of complications (36) and being associated with adverse outcomes (19, 38, 39). It remains unknown if the adverse outcomes are related to the conformational changes in the wrist. During carpal distraction, the ideal goal is to localize the effect of ligamentotaxis to the radiocarpal joint (36). Based on our results, it is important to realize that during distraction there is greater separation taking place at the

midcarpal joint than at the radiocarpal joint. Using the radiolunate and lunocapitate joints as representative joints, there is 2.0 times the separation taking place at the midcarpal joint as compared to the radiocarpal joint. If the goal of ligamentotaxis is to align the distal radius (18), surgeons should be aware that changes at the midcarpal joint are significantly greater than at the radiocarpal joint and there is a risk of damaging ligaments if too much force is applied (37).

Wrist distraction may not be useful as a diagnostic tool for scapholunate ligament injury. Wrist distraction is also used clinically to test for injury to the scapholunate ligament (12, 13). Using the “carpal stress test” (12), with the wrist placed under 5kg (49N) distraction; a visible stepoff can be seen on a posteroanterior radiograph of patients with an scapholunate ligament injury. Our results suggest that surgeons must be careful using this technique alone for diagnosis. In healthy subjects, we found that the scaphoid distracted axially 2.4 times further than the lunate. It is challenging to apply our findings to the clinical setting because we are estimating the view as seen on an anteroposterior radiograph and we are looking at translation of the centroid only, whereas the stepoff measurement relies on measuring the distances between the bone edges as seen on the radiograph. Additionally, the load in the “carpal stress test” is applied only to the thumb and index finger, whereas our load was applied to all 5 fingers. While the reported distractive load (49N) in their study is half of our load (98N), the actual loads across the carpus might be closer. Our distractive load was applied directly to the finger traps with the arm in the horizontal position. In their study, the arm was suspended from the finger traps, with a 98N load attached to the arm; thus the load across the carpus include the weight of the forearm and the 49N applied load.

A second study found that an increase in scapholunate distance of at least 1.0mm as a function of 5kg (49N) of distractive loading was indicative of a scapholunate ligament tear (13). In this study the wrist was suspended from only the thumb, and the carpal load was again the combined weight of the forearm and 49N load. Our results correlate with this study, as we saw less than 0.1mm change in the scaphoid-lunate centroid distance.

One limitation of using an *in vivo* method is the challenge of maintaining a consistent wrist position between the unloaded and loaded trial. By loaded each volunteer before the unloaded trial and keeping the interval between scans as short as possible, we attempted to minimize the variation in wrist position. While there remained an average difference of 6° between the unloaded and loaded position, achieving greater consistency would require a complex jig that could alter the biomechanics we are trying to measure.

Though our findings were significant, it is possible that our data actually under-represented what normally occurs during wrist distraction. While we asked our volunteers to relax during loading, and attempted to confirm this through palpation, it is possible that some volunteers partially resisted the loading via forearm muscle contraction. The somewhat large standard deviation values suggest that there were subjects for whom there was minimal distraction and others of whom distracted more than our reported averages.

In summary, this study provides insight into the mechanical behavior of the ligamentous carpus, which to date is scant in the literature. The results of this study can be used when generating computer models of the wrist (40, 41). Similarly, the data can

also be used to validate a cadaver model, which could then be used for studying various pathologic states.

3.6 References

1. Berger, R.A., *The ligaments of the wrist. A current overview of anatomy with considerations of their potential functions.* Hand Clin, 1997. **13**(1): 63-82.
2. Nanno, M., Patterson, R.M., and Viegas, S.F., *Three-dimensional imaging of the carpal ligaments.* Hand Clin, 2006. **22**(4): 399-412; abstract v.
3. Nowalk, M.D. and Logan, S.E., *Distinguishing biomechanical properties of intrinsic and extrinsic human wrist ligaments.* J Biomech Eng, 1991. **113**(1): 85-93.
4. Viegas, S.F., *The dorsal ligaments of the wrist.* Hand Clin, 2001. **17**(1): 65-75, vi.
5. Mayfield, J., *Pathogenesis of Wrist Ligament Instability*, in *The Wrist and its Disorders*, Lichtman, D., Editor. 1988, WB Saunders: Philadelphia. p. 53-73.
6. Mitsuyasu, H., Patterson, R.M., Shah, M.A., Buford, W.L., Iwamoto, Y., and Viegas, S.F., *The role of the dorsal intercarpal ligament in dynamic and static scapholunate instability.* J Hand Surg [Am], 2004. **29**(2): 279-288.
7. Short, W.H., Werner, F.W., Fortino, M.D., Palmer, A.K., and Mann, K.A., *A dynamic biomechanical study of scapholunate ligament sectioning.* J Hand Surg [Am], 1995. **20**(6): 986-999.
8. Short, W.H., Werner, F.W., Green, J.K., Weiner, M.M., and Masaoka, S., *The effect of sectioning the dorsal radiocarpal ligament and insertion of a pressure sensor into the radiocarpal joint on scaphoid and lunate kinematics.* J Hand Surg [Am], 2002. **27**(1): 68-76.
9. Moritomo, H., Murase, T., Arimitsu, S., Oka, K., Yoshikawa, H., and Sugamoto, K., *Change in the length of the ulnocarpal ligaments during radiocarpal motion: possible impact on triangular fibrocartilage complex foveal tears.* J Hand Surg [Am], 2008. **33**(8): 1278-1286.
10. Marai, G.E., Laidlaw, D.H., Demiralp, C., Andrews, S., Grimm, C.M., and Crisco, J.J., *Estimating joint contact areas and ligament lengths from bone kinematics and surfaces.* IEEE Trans Biomed Eng, 2004. **51**(5): 790-799.
11. Loebig, T.G., Badia, A., Anderson, D.D., and Baratz, M.E., *Correlation of wrist ligamentotaxis with carpal distraction: implications for external fixation.* J Hand Surg [Am], 1997. **22**(6): 1052-1056.
12. Yamaguchi, S., Beppu, M., Matsushita, K., and Takahashi, K., *The carpal stretch test at the scapholunate joint.* J Hand Surg [Am], 1998. **23**(4): 617-625.
13. Schadel-Hopfner, M., Bohringer, G., Gotzen, L., and Celik, I., *Traction radiography for the diagnosis of scapholunate ligament tears.* J Hand Surg [Br], 2005. **30**(5): 464-467.
14. Ishikawa, J., Cooney, W.P., 3rd, Niebur, G., An, K.N., Minami, A., and Kaneda, K., *The effects of wrist distraction on carpal kinematics.* J Hand Surg [Am], 1999. **24**(1): 113-120.
15. Larsson, L.G., Baum, J., and Mudholkar, G.S., *Hypermobility: features and differential incidence between the sexes.* Arthritis Rheum, 1987. **30**(12): 1426-1430.

16. Shultz, S.J., Shimokochi, Y., Nguyen, A.D., Schmitz, R.J., Beynnon, B.D., and Perrin, D.H., *Measurement of varus-valgus and internal-external rotational knee laxities in vivo--Part II: relationship with anterior-posterior and general joint laxity in males and females*. J Orthop Res, 2007. **25**(8): 989-996.
17. Scerpella, T.A., Stayer, T.J., and Makhuli, B.Z., *Ligamentous laxity and non-contact anterior cruciate ligament tears: a gender-based comparison*. Orthopedics, 2005. **28**(7): 656-660.
18. Agee, J.M., *Distal radius fractures. Multiplanar ligamentotaxis*. Hand Clin, 1993. **9**(4): 577-585.
19. Kaempffe, F.A., Wheeler, D.R., Peimer, C.A., Hvidsak, K.S., Ceravolo, J., and Senall, J., *Severe fractures of the distal radius: effect of amount and duration of external fixator distraction on outcome*. J Hand Surg [Am], 1993. **18**(1): 33-41.
20. Fortems, Y., Mawhinney, I., Lawrence, T., and Stanley, J.K., *Traction radiographs in the diagnosis of chronic wrist pain*. J Hand Surg [Br], 1994. **19**(3): 334-337.
21. Crisco, J.J., Coburn, J.C., Moore, D.C., and Upal, M.A., *Carpal bone size and scaling in men versus in women*. J Hand Surg [Am], 2005. **30**(1): 35-42.
22. Trumble, T., Glisson, R.R., Seaber, A.V., and Urbaniak, J.R., *Forearm force transmission after surgical treatment of distal radioulnar joint disorders*. J Hand Surg [Am], 1987. **12**(2): 196-202.
23. Kazuki, K., Kusunoki, M., and Shimazu, A., *Pressure distribution in the radiocarpal joint measured with a densitometer designed for pressure-sensitive film*. J Hand Surg [Am], 1991. **16**(3): 401-408.
24. Hara, T., Horii, E., An, K.N., Cooney, W.P., Linscheid, R.L., and Chao, E.Y., *Force distribution across wrist joint: application of pressure-sensitive conductive rubber*. J Hand Surg [Am], 1992. **17**(2): 339-347.
25. Kobayashi, M., Garcia-Elias, M., Nagy, L., Ritt, M.J., An, K.N., Cooney, W.P., and Linscheid, R.L., *Axial loading induces rotation of the proximal carpal row bones around unique screw-displacement axes*. J Biomech, 1997. **30**(11-12): 1165-1167.
26. Coburn, J.C., Upal, M.A., and Crisco, J.J., *Coordinate systems for the carpal bones of the wrist*. J Biomech, 2007. **40**(1): 203-209.
27. Gonzalez-Ochoa, C., McCammon, S., and Peters, J., *Computing Moments of Objects Enclosed by Piecewise Polynomial Surfaces*. ACM Transactions on Graphics (TOG), 1998. **17**(3): 143-157.
28. Crisco, J.J., McGovern, R.D., and Wolfe, S.W., *Noninvasive technique for measuring in vivo three-dimensional carpal bone kinematics*. J Orthop Res, 1999. **17**(1): 96-100.
29. Marai, G.E., Laidlaw, D.H., and Crisco, J.J., *Super-resolution registration using tissue-classified distance fields*. IEEE Trans Med Imaging, 2006. **25**(2): 177-187.
30. Moritomo, H., Murase, T., Goto, A., Oka, K., Sugamoto, K., and Yoshikawa, H., *In vivo three-dimensional kinematics of the midcarpal joint of the wrist*. J Bone Joint Surg Am, 2006. **88**(3): 611-621.
31. Wolfe, S.W., Neu, C., and Crisco, J.J., *In vivo scaphoid, lunate, and capitate kinematics in flexion and in extension*. J Hand Surg [Am], 2000. **25**(5): 860-869.
32. Taleisnik, J., *The ligaments of the wrist*. J Hand Surg [Am], 1976. **1**(2): 110-118.

33. Mayfield, J.K., Johnson, R.P., and Kilcoyne, R.F., *The ligaments of the human wrist and their functional significance*. Anat Rec, 1976. **186**(3): 417-428.
34. Mayfield, J.K., Williams, W.J., Erdman, A.G., Dahlof, W.J., Wallrich, M.A., Kleinhenz, W.A., and Moody, N.R., *Biomechanical properties of human carpal ligaments*. Orthop. Trans., 1979. **3**(2): 143-144.
35. Neu, C.P., Crisco, J.J., and Wolfe, S.W., *In vivo kinematic behavior of the radio-capitate joint during wrist flexion-extension and radio-ulnar deviation*. J Biomech, 2001. **34**(11): 1429-1438.
36. Biyani, A., *Over-distraction of the radio-carpal and mid-carpal joints following external fixation of comminuted distal radial fractures*. J Hand Surg [Br], 1993. **18**(4): 506-510.
37. Bartosh, R.A. and Saldana, M.J., *Intraarticular fractures of the distal radius: a cadaveric study to determine if ligamentotaxis restores radiopalmar tilt*. J Hand Surg [Am], 1990. **15**(1): 18-21.
38. Kaempffe, F.A., *External fixation for distal radius fractures: adverse effects of excess distraction*. Am J Orthop, 1996. **25**(3): 205-209.
39. Kaempffe, F.A. and Walker, K.M., *External fixation for distal radius fractures: effect of distraction on outcome*. Clin Orthop Relat Res, 2000(380): 220-225.
40. Iwasaki, N., Genda, E., Minami, A., Kaneda, K., and Chao, E.Y., *Force transmission through the wrist joint in Kienbock's disease: a two-dimensional theoretical study*. J Hand Surg [Am], 1998. **23**(3): 415-424.
41. Carrigan, S.D., Whiteside, R.A., Pichora, D.R., and Small, C.F., *Development of a three-dimensional finite element model for carpal load transmission in a static neutral posture*. Ann Biomed Eng, 2003. **31**(6): 718-725.

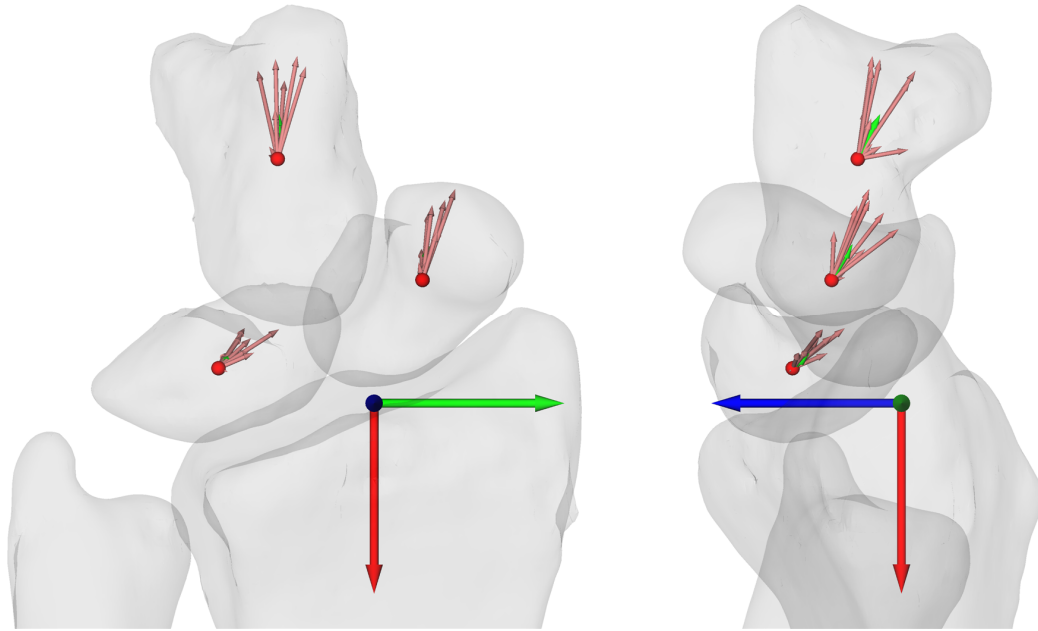


Figure 3.1. Volar (left) and Radial (right) view of a single subject's wrist showing the radius, ulna, scaphoid, lunate and capitate. The centroid (red) for each carpal bone in the unloaded position, and the centroid displacement for each subject (light red) showing the translation of the subject as a function of loading. The vector representing average translation with loading is shown in green.

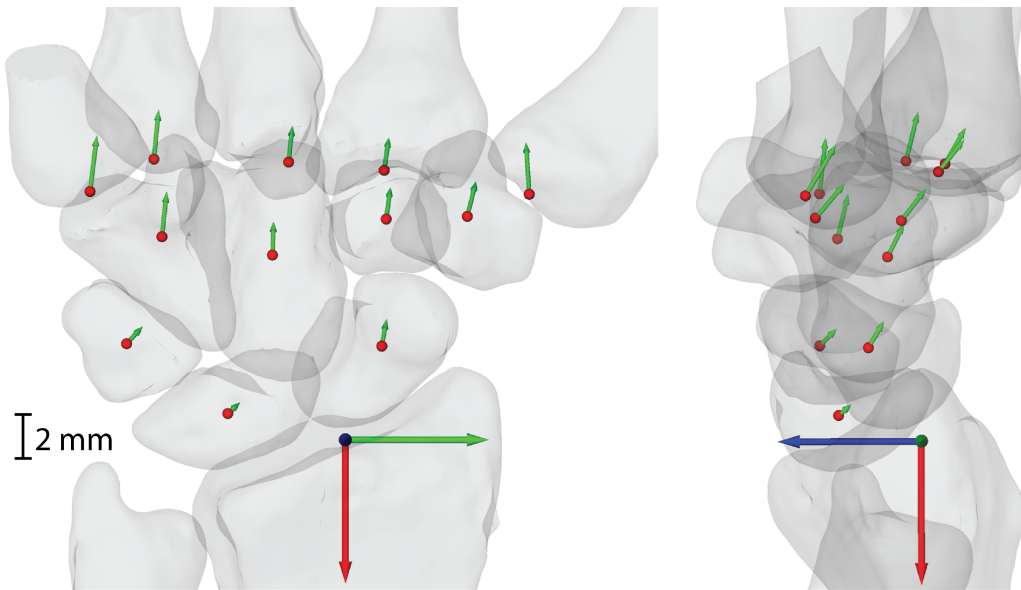


Figure 3.2. Volar (left) and Radial (right) view of a single wrist showing the centroid (red sphere) of each bone in the unloaded position and a vector representing the average centroid displacement after loading.

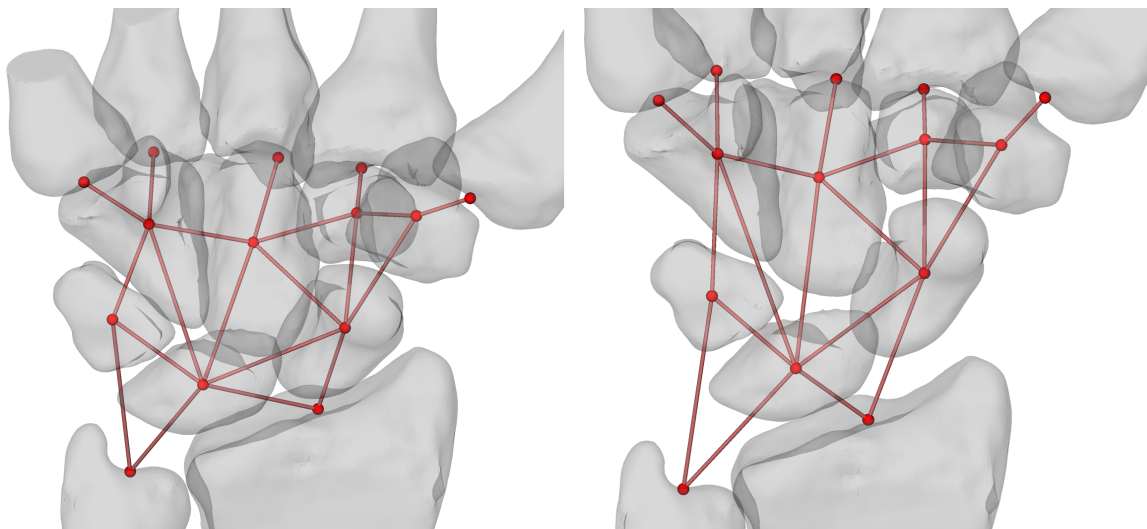


Figure 3.3. Volar view of a single wrist in the unloaded (left) and loaded (right) state. The centroid of each bone is shown (red sphere). Intercentroid combinations that were analyzed are represented as lines connecting the two bone centroids. There is visible distraction at the radiocarpal and midcarpal joints.

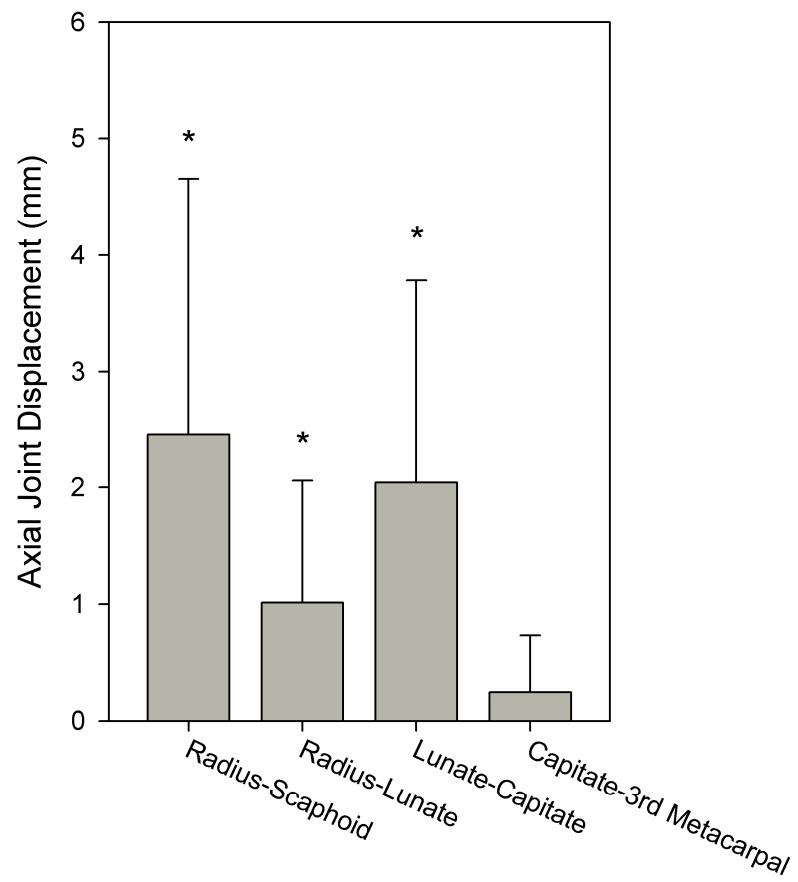


Figure 3.4. Tensive loading caused a significant (*) increase in the interbone distances at the radioscaphoid, radiolunate and lunocapitate joints. There was a non-significant increase in the interbone distance at the 3rd carpal-metacarpal joint.

<i>Bone</i>	<i>Bone</i>	<i>Change in Centroid Distance (mm)</i>
Radius	Lunate	-1.02 ± 1.0
Lunate	Triquetrum	-0.07 ± 0.1
Trapezium	Trapezoid	-0.06 ± 0.1
Trapezoid	2nd Metacarpal	0.05 ± 0.2
Lunate	Scaphoid	0.08 ± 0.5
Capitate	Hamate	0.09 ± 0.1
Trapezium	1st Metacarpal	0.12 ± 0.4
Capitate	Trapezoid	0.20 ± 0.2
Hamate	4th Metacarpal	0.22 ± 0.3
Scaphoid	Trapezium	0.25 ± 0.5
Capitate	3rd Metacarpal	0.27 ± 0.2
Scaphoid	Trapezoid	0.43 ± 1.0
Hamate	5th Metacarpal	0.58 ± 0.4
Scaphoid	Capitate	0.58 ± 0.8
Ulna	Lunate	1.06 ± 1.3
Ulna	Triquetrum	1.20 ± 1.5
Lunate	Capitate	1.64 ± 1.4
Radius	Scaphoid	1.80 ± 2.0
Hamate	Triquetrum	2.13 ± 1.4
Lunate	Hamate	2.95 ± 1.9

Table 3.1. Bone-bone interactions were measured as the change in distance between centroids after loading.

<i>Bone</i>	<i>Centroid Displacement (mm)</i>	<i>Direction of Translation Vector</i>	
		<i>Dorsal (°)</i>	<i>Radial (°)</i>
Scaphoid	3.11 ± 2.5	30.5	8.7
Lunate	2.19 ± 1.7	48.8	36.1
Triquetrum	2.93 ± 1.9	44.9	33.6
Trapezoid	4.20 ± 2.9	37.9	6.1
Trapezium	4.74 ± 3.0	40.5	10.6
Capitate	3.75 ± 2.6	26.7	1.8
Hamate	4.67 ± 2.7	13.7	5.9
1st Metacarpal	6.06 ± 3.4	31.0	-3.1
2nd Metacarpal	4.48 ± 3.0	38.7	6.3
3rd Metacarpal	4.49 ± 2.8	29.8	5.1
4th Metacarpal	5.36 ± 3.0	13.9	5.3
5th Metacarpal	5.89 ± 3.0	6.3	7.0

Table 3.2. Translation vectors were calculated for each bone centroid representing its translation after loading. These vectors were represented as both a magnitude and by the orientation of the vector.

Chapter 4

Conclusions & Future Directions

4.1 Conclusions

Our goal was to gain a better understanding of one of the most complicated joints in the human body: the wrist. The majority of past carpal research has been focused on understanding the behavior of the unloaded wrist during orthogonal motions. Unfortunately, the human wrist routinely moves in non-orthogonal motions and is subject to various loads. The goal of this research was to examine the wrist during motions that better represent activities of daily living.

Specifically, this research had two primary objectives: 1) To examine the motion of the wrist and forearm during hammering, and to determine the *in vivo* three-dimensional carpal kinematics during this functional task; 2) To measure the *in vivo* three-dimensional changes in the healthy carpus as the result of a static distractive load.

In chapter 2, we set out to examine the kinematics of the wrist and forearm during a simulated hammering motion. We chose hammering to represent a functional task presumed to use the DTM. Our results showed that hammering used a combined motion of ulnar flexion. Forearm pronation/supination was minimal, averaging only 12° of

rotation throughout the full hammering motion. Although scaphoid and lunate rotations were measured at 40% of overall wrist motion during hammering, instead of the roughly 0% predicted, this was still a large reduction compared to pure flexion/extension. The direction of wrist motion used during hammering was shown to affect the magnitude of radiocarpal rotation.

Chapter 3 focused on the *in vivo* wrist under distractive loading. After applying 98N of distractive force to the right wrist of 14 healthy volunteers, we measured an average of 3.3mm distraction across the entire carpus (radius to 3rd metacarpal). The largest separation took place at the midcarpal joint (lunate to capitate), followed by the radiocarpal joint (radius to lunate). These findings should serve as warnings to surgeons who use carpal distraction for the treatment of distal radial fractures (1). Surgeons must be aware that their distractive loads have effects beyond the radiocarpal joint, and that distraction affects the midcarpal joint almost twice as much as the radiocarpal joint. Similarly, the use of distraction to assess the integrity of the scapholunate interosseous ligament (2, 3) should be carefully considered. In our healthy volunteers, we found that the scaphoid distracted almost 2.5 times further than the lunate. While we were unable to offer a clear mechanism for these changes, our findings have practical applications for designing computer models as well as validating a cadaver model which can be used to more easily test the effects of various injuries.

In chapters 2 and 3, we continue a long history of the study of carpal kinematics. While this research has not revealed the key to developing a comprehensive model of carpal kinematics, it has brought us closer to this goal.

4.1.1 What is the Dart Throwing Motion?

One of the difficulties encountered during this research was that the fact that the DTM remains poorly defined despite a surge in interest. There is no universally accepted path of motion, nor is there a precise definition of the DTM. The most liberal definitions define the DTM as any path of motion between the arc of pure flexion and pure ulnar deviation. This definition creates an infinite number of possible DTM paths over an arc of 90° . Further, that arc includes almost half of the possible paths of wrist motion.

In a 2007 consensus paper written by Moritomo et al. (4), the DTM was defined as: "...a plane in which wrist functional oblique motion occurs, specifically from radial extension to ulnar flexion." The authors also state that, "During a DTM there is less scaphoid and lunate motion than during pure flexion-extension or radioulnar deviation."

In trying to understand the DTM, a number of important questions arose. The first question: *For a given individual, is the DTM a single path or is it a collection of paths?* If the DTM is described as a collection of paths, then it is important to narrow the arc from the broadest 90° arc. At 90° , studying the DTM becomes almost synonymous with simply studying carpal kinematics.

Using the singular expression in the name "Dart Throwing *Motion*" for guidance, even more questions are raised when trying to define a single DTM path for an individual. If the DTM is a single path, then is it: 1) a functional path of motion? 2) the path which minimizes radioscapoid rotation? 3) the path which minimizes radiolunate rotation? There is reasonable evidence to suggest that no single path can meet all three definitions; furthermore, it is unclear if there is any clinical difference between those definitions.

In chapter 2 we discussed how the results of two previous studies as well as our own suggest that the paths which minimize radioscapoid and radiolunate rotation differ by approximately 12° . It is also likely that there is no single functional motion, although the most functional tasks might happen using a narrow arc of wrist motion. The lack of a single functional path of motion is supported by prior work has shown that hammering and dart throwing, two prototypical examples of tasks which utilize the DTM, involve different paths of wrist motion (5). Similarly, past studies have demonstrated that the wrist motion can vary depending upon the type of hammering being performed (6).

4.1.2 Intersubject variability

Regardless of the definition used, it is likely that there are differences in the DTM between subjects (4, 7). This is not unexpected giving that there is known variation in the morphology of the human carpus. For example, there is a well established classification for type I and type II lunates, depending upon if they have an articulation with the hamate (8). Similarly, there have been various attempts to create a similar type of classification for the scaphoid (9) and possibly the capitate (10). What remains unknown is if these different bone shapes cause variations in carpal kinematics. Preliminary work has shown that it might be possible to detect these differences. One group was able to detect slight differences in the motion of type I and type II lunates using 2-D analysis of 10 patients (11).

An understanding of the morphologic variations of the wrist could assist in the diagnosis and treatment of disease. For example, it has been established that individuals with type II lunates have a higher rate of arthrosis at the lunohamate joint (12), although

those same individuals are less likely to have dorsal intercalated segment instability (DISI) with scaphoid nonunion (13).

4.2 Future Methods for Non-Invasively Measuring 3-D Carpal Kinematics

4.2.1 Current Research Methodologies

Accurately studying carpal kinematics is fraught with technical challenges. The small size of the carpal bones and the vast number of articulations, make analysis using conventional methods almost impossible. Historically, carpal studies have been performed using surface markers, invasive markers, or plain radiographs. Unfortunately each method suffers from significant limitations such as being unable to measure the kinematics of individual carpal bones or possibly altering the kinematics they are trying to measure. Cadaver models have been used in many studies, but there are inherent limitations to these models. Cadaveric models lack normal muscle tone, and can be contaminated by various existing pathologies due to the age of most specimens.

In these studies we chose to use a CT based markerless registration methodology (14, 15) for tracking the 3-D motions of the carpus. There are significant limitations associated with a CT based method. Like any x-ray based imaging, there is radiation exposure for the volunteers; however, this risk is minimized by using lower power settings on the CT scanner and providing volunteers with the appropriate level of protection. Using CT scans requires that we collect images from static postures, complicating our understanding of the dynamic motion of the wrist. Radiation exposure limits us to only 12 scans per volunteer resulting in only a handful of data points per subject.

Despite these limitations, our CT based method has important advantages over the alternatives. Methods using surface markers or external devices are unable to measure the motion of individual carpal bones rendering them inappropriate for our studies. Invasive pins and markers have been used both *in vivo* and *in vitro*, however, these methods can alter the motions we are trying to measure and pose additional challenges when recruiting study volunteers.

Currently, an MRI based system (16, 17) is the only other way to non-invasively measure the kinematics of the carpus. While MRI does not have the radiation exposure associated with CT scans, individual scans take considerably longer to acquire and the method has been shown to be less accurate than CT imaging.

4.2.2 Future Imaging Modalities

While the options for successfully studying carpal kinematics are currently limited, technology continues to move forward and new methods are always being developed. There has been recent work to try and capture CT scans in real time (18), however this technology is still under development and its accuracy has not been established.

Another possible method for studying carpal kinematics is the use of a combination of CT and dual fluoroscopes, known as XROMM (X-Ray Reconstruction Of Moving Morphology). In XROMM, a single CT scan of the joint in a static position is first acquired. Motion is then recorded using two fluoroscopes, which create two distinct views of the scene. A computer algorithm creates a variety of projections of each bone in the CT scan and compares the projections to each frame of the video acquired from the

fluoroscopes. Through an iterative process, the algorithm determines the most likely orientation for each bone in the two views. Combining the known positions of the two fluoroscopes, and the orientation of each bone in the videos, it is possible to compute the position of each bone in 3-D space. The strength of such a technique is the ability to measure dynamic motions, and analyze the kinematics throughout a range of motion.

While similar technology has been used in larger joints such as the knee for many years (19), there are still numerous challenges associated with the use of XROMM in the wrist due to its smaller and more numerous bones. Pilot data has shown that the bones of the foot can be tracked using implanted markers; however, the creation of a system for markerless tracking is in preliminary stages. Further, even though the foot is considerably harder to track than the knee, the wrist may prove to be even more challenging as the bones of this joint are much smaller and more closely arranged. XROMM potentially offers an incredibly powerful non-invasive modality for capturing the kinematics of the carpus at extremely high frame rate if the technical challenges are overcome.

4.3 Future Directions

4.3.1 Correlations Between Morphology and Kinematics

While there are variations in carpal morphology, it is largely unknown how these variations affect carpal kinematics. Understanding these differences could profoundly impact how the wrist is studied in the future. There are significant challenges associated with performing such a study, as the variation between different wrist types are likely quite small and would require a high sample number. This is further complicated, by the fact that the lunate is the only carpal bone with a well defined morphological classification system. Despite these challenges, one group has already shown slight differences in motion between individuals with type I and type II lunates (11).

The first step should include the creation of a classification system for the carpal bones. These classifications must be objectively determined. The next step would be to establish if there was a correlation between different bone shapes, and ideally come up with a classification for the entire wrist. The final challenge lies in trying to determine kinematic differences between those classifications.

Fortunately, in addition to the lunate, classification systems for the scaphoid and capitate have already been proposed (9, 10). Additionally, our lab has an extensive database of carpal kinematics (20), consisting of accurate 3-D bone models, and kinematics for at least 64 healthy subjects in 1048 wrist positions. This database could provide an incredible resource for identifying possible differences in kinematics between wrist types.

4.3.2 High Accuracy Study of a Single Specimen

Historically, our wrist studies have used multiple subjects scanned in 8 to 12 wrist positions. One limitation of this approach is that we have only a limited amount of information for each individual and our reported results are often averaged across subjects in various positions. It would be useful to eliminate the intersubject variability, by collecting a far larger number of positions using fewer subjects. While it is preferable to use an *in vivo* model, the high number of scans creates an unacceptable level of radiation exposure, thus requiring a cadaver model.

By collecting data for various DTM paths at a high sampling frequency, it might be possible to answer various questions regarding this motion. Specifically, how the flexion/extension offset of the wrist impacts radiocarpal motion, what the exact path of motion is that minimizes scaphoid and lunate rotation, and what the minimum amount of radiocarpal rotation is. To take the study even further, we would sample as many wrist positions as feasible, including those outside the previously described DTM paths. Doing so could allow better approximations of any path of motion in the wrist.

The proposed study would not be terribly hard to perform for a variety of reasons. Normally, the majority of time spent on data collection involves setting up the experiment and cleaning up after. Newer CT scanners have considerably reduced the time required for scanning, allowing for a greater number of scans that can be collected. By reducing the number of subjects, the amount of time spent manually segmenting is vastly reduced, as segmentation is only performed once per subject. The final time consuming part of generating carpal data has been the semi-automated registration process. Fortunately, advances in storage and computing power have again reduced the

amount of time required for this process. If the XROMM technology proves to be applicable to the wrist, it might be possible to perform this study *in vivo* using dynamic motions, which could prove even more useful.

4.4 Ongoing Loading Studies

In addition to our tensile loading task (chapter 3), we collected data from the same 14 volunteers during two additional loading studies. The first was another tensile loading task; however, for this second tensile task volunteers held the load using grip, thereby activating their forearm muscles. The second was a compressive task simulating a pushup. Both tasks were performed without load and under the same 98N load used in chapter 3.

4.4.1 Tensile Gripping Task

4.4.1.1 Background

Our distractive task in chapter 3 was chosen based on its clinical relevance; however, few individuals lift items using finger traps during normal activities of daily living. This tensile gripping trial was designed to better represent the loads that are seen across the carpus when an object is carried using a handle as opposed to finger traps. Under these conditions, the forearm muscles are activated to close the fingers and maintain a grip on the handle. It is unknown how activation of the forearm muscles affects the conformation of the carpus.

As previously discussed, there are only a limited number of studies that investigated the carpus under tensile distraction (21, 22). Studies of the wrist have been performed on the so-called “power-grip” (23-26), however, these studies do not utilize external loads. There are no published studies on the wrist under tensile load while

gripping. The purpose of this experiment was to measure the 3-D changes in the healthy carpus during tensive loading of the wrist with active gripping.

4.4.1.2 Data Collection

The gripping task was performed using a protocol similar to that used in the distraction study discussed in chapter 3, using the same 14 volunteers. The principal difference between the two tasks was how volunteers were asked to carry the load. Instead of using finger traps, volunteers were asked to hold the weight using a radiotranslucent handle. By grasping a handle to carry the load, volunteers were required to activate the muscles of the forearm. Prior to the unloaded trial, the handle was briefly loaded to allow the wrist to assume its natural position under load and minimize variations in wrist posture between the loaded and unloaded state. The same 98N (or 10kg) load was used for the loaded trial.

4.4.2 Compressive Task

4.4.2.1 Background

Several studies have tried to measure contact pressure and area at the radiocarpal joint *in vitro* using various types of sensors (27-29). These studies established that joint contact at the radiocarpal joint was approximately 20% of overall joint surface. One study tested a custom sensor *in vivo* in a single healthy volunteer (30) as a proof of concept, but additional work using this technique has not been reported.

Carpal kinematics during compression was measured in a single cadaveric study (31). Applying 98N of compressive loading caused minimal scaphoid (5.1°) and lunate (4.2°) rotation. These results are hard to extrapolate to the *in vivo* carpus because of the artificial constraint on wrist motion as well as the non-physiologic distribution of force among the tendons of the wrist. Our study was designed to enable us to measure these changes *in vivo* and eliminate many of these confounding factors.

The purpose of this final task was to measure the 3-D changes in carpal kinematics during compressive loading of the extended wrist.

4.4.2.2 Data Collection

For compressive loading, a standard bathroom scale was mounted vertically in a custom jig. Volunteers were positioned with their palm centered on the scale and their forearm perpendicular to the surface of the scale. Unlike the tensive tasks (chapter 3 & 4.4), where the load was applied by deadweight, the loaded trial of the compressive task required that each volunteer apply a force against the scale and hold that position. By using a standard bathroom scale, volunteers had immediate feedback as to how much force they applied during the loaded trial. Informal experimentation with this setup in our lab showed that with proper instruction, it was not difficult to apply the 98N force and remain motionless for the short duration of a scan. Care was taken to ensure that their hand, elbow and shoulder were aligned down the center of the scanning table. Images were acquired in both the unloaded (0N) state and the loaded state (98N).

4.5 References

1. Agee, J.M., *Distal radius fractures. Multiplanar ligamentotaxis*. Hand Clin, 1993. **9**(4): 577-585.
2. Schadel-Hopfner, M., Bohringer, G., Gotzen, L., and Celik, I., *Traction radiography for the diagnosis of scapholunate ligament tears*. J Hand Surg [Br], 2005. **30**(5): 464-467.
3. Yamaguchi, S., Beppu, M., Matsushita, K., and Takahashi, K., *The carpal stretch test at the scapholunate joint*. J Hand Surg [Am], 1998. **23**(4): 617-625.
4. Moritomo, H., Apergis, E.P., Herzberg, G., Werner, F.W., Wolfe, S.W., and Garcia-Elias, M., *2007 IFSSH committee report of wrist biomechanics committee: biomechanics of the so-called dart-throwing motion of the wrist*. J Hand Surg [Am], 2007. **32**(9): 1447-1453.
5. Curan, P.F., Rainbow, M.J., Moore, D.C., and Crisco, J.J. *Hammering and Dart Throwing are Kinetically Different*. in American Society of Biomechanics. 2007. Stanford University, Stanford, CA.
6. Schoenmarklin, R.W. and Marras, W.S., *Effects of handle angle and work orientation on hammering: I. Wrist motion and hammering performance*. Hum Factors, 1989. **31**(4): 397-411.
7. Crisco, J.J., Coburn, J.C., Moore, D.C., Akelman, E., Weiss, A.P., and Wolfe, S.W., *In vivo radiocarpal kinematics and the dart thrower's motion*. J Bone Joint Surg Am, 2005. **87**(12): 2729-2740.
8. Viegas, S.F., Wagner, K., Patterson, R., and Peterson, P., *Medial (hamate) facet of the lunate*. J Hand Surg [Am], 1990. **15**(4): 564-571.
9. Heinzlmann, A.D., Archer, G., and Bindra, R.R., *Anthropometry of the human scaphoid*. J Hand Surg [Am], 2007. **32**(7): 1005-1008.
10. Yazaki, N., Burns, S.T., Morris, R.P., Andersen, C.R., Patterson, R.M., and Viegas, S.F., *Variations of capitate morphology in the wrist*. J Hand Surg [Am], 2008. **33**(5): 660-666.
11. Nakamura, K., Beppu, M., Patterson, R.M., Hanson, C.A., Hume, P.J., and Viegas, S.F., *Motion analysis in two dimensions of radial-ulnar deviation of type I versus type II lunates*. J Hand Surg [Am], 2000. **25**(5): 877-888.
12. Nakamura, K., Patterson, R.M., Moritomo, H., and Viegas, S.F., *Type I versus type II lunates: Ligament anatomy and presence of arthrosis*. J Hand Surg [Am], 2001. **26**(3): 428-436.
13. Haase, S.C., Berger, R.A., and Shin, A.Y., *Association between lunate morphology and carpal collapse patterns in scaphoid nonunions*. J Hand Surg [Am], 2007. **32**(7): 1009-1012.
14. Crisco, J.J., McGovern, R.D., and Wolfe, S.W., *Noninvasive technique for measuring in vivo three-dimensional carpal bone kinematics*. J Orthop Res, 1999. **17**(1): 96-100.
15. Marai, G.E., Laidlaw, D.H., and Crisco, J.J., *Super-resolution registration using tissue-classified distance fields*. IEEE Trans Med Imaging, 2006. **25**(2): 177-187.

16. Moritomo, H., Murase, T., Goto, A., Oka, K., Sugamoto, K., and Yoshikawa, H., *Capitate-based kinematics of the midcarpal joint during wrist radioulnar deviation: an in vivo three-dimensional motion analysis*. J Hand Surg [Am], 2004. **29**(4): 668-675.
17. Moritomo, H., Goto, A., Sato, Y., Sugamoto, K., Murase, T., and Yoshikawa, H., *The triquetrum-hamate joint: an anatomic and in vivo three-dimensional kinematic study*. J Hand Surg [Am], 2003. **28**(5): 797-805.
18. Tay, S.C., Primak, A.N., Fletcher, J.G., Schmidt, B., Amrami, K.K., Berger, R.A., and McCollough, C.H., *Four-dimensional computed tomographic imaging in the wrist: proof of feasibility in a cadaveric model*. Skeletal Radiol, 2007. **36**(12): 1163-1169.
19. You, B.M., Siy, P., Anderst, W., and Tashman, S., *In vivo measurement of 3-D skeletal kinematics from sequences of biplane radiographs: application to knee kinematics*. IEEE Trans Med Imaging, 2001. **20**(6): 514-525.
20. Moore, D.C., Crisco, J.J., Trafton, T.G., and Leventhal, E.L., *A digital database of wrist bone anatomy and carpal kinematics*. J Biomech, 2007. **40**(11): 2537-2542.
21. Ishikawa, J., Cooney, W.P., 3rd, Niebur, G., An, K.N., Minami, A., and Kaneda, K., *The effects of wrist distraction on carpal kinematics*. J Hand Surg [Am], 1999. **24**(1): 113-120.
22. Loebig, T.G., Badia, A., Anderson, D.D., and Baratz, M.E., *Correlation of wrist ligamentotaxis with carpal distraction: implications for external fixation*. J Hand Surg [Am], 1997. **22**(6): 1052-1056.
23. Fong, P.W. and Ng, G.Y., *Effect of wrist positioning on the repeatability and strength of power grip*. Am J Occup Ther, 2001. **55**(2): 212-216.
24. Garcia-Elias, M., *Kinetic analysis of carpal stability during grip*. Hand Clin, 1997. **13**(1): 151-158.
25. LaStayo, P. and Hartzel, J., *Dynamic versus static grip strength: how grip strength changes when the wrist is moved, and why dynamic grip strength may be a more functional measurement*. J Hand Ther, 1999. **12**(3): 212-218.
26. Morse, J.L., Jung, M.C., Bashford, G.R., and Hallbeck, M.S., *Maximal dynamic grip force and wrist torque: the effects of gender, exertion direction, angular velocity, and wrist angle*. Appl Ergon, 2006. **37**(6): 737-742.
27. Viegas, S.F. and Patterson, R.M., *Load mechanics of the wrist*. Hand Clin, 1997. **13**(1): 109-128.
28. Kazuki, K., Kusunoki, M., and Shimazu, A., *Pressure distribution in the radiocarpal joint measured with a densitometer designed for pressure-sensitive film*. J Hand Surg [Am], 1991. **16**(3): 401-408.
29. Rikli, D.A., Honigmann, P., Babst, R., Cristalli, A., Morlock, M.M., and Mittlmeier, T., *Intra-articular pressure measurement in the radioulnocarpal joint using a novel sensor: in vitro and in vivo results*. J Hand Surg [Am], 2007. **32**(1): 67-75.
30. Hara, T., Horii, E., An, K.N., Cooney, W.P., Linscheid, R.L., and Chao, E.Y., *Force distribution across wrist joint: application of pressure-sensitive conductive rubber*. J Hand Surg [Am], 1992. **17**(2): 339-347.

31. Kobayashi, M., Garcia-Elias, M., Nagy, L., Ritt, M.J., An, K.N., Cooney, W.P., and Linscheid, R.L., *Axial loading induces rotation of the proximal carpal row bones around unique screw-displacement axes*. J Biomech, 1997. **30**(11-12): 1165-1167.